Applied Microbiology and Biotechnology (2023) 107:749–768
https://doi.org/10.1007/s00253-022-12312-3

APPLIED GENETICS AND MOLECULAR BIOTECHNOLOGY

Genomic analysis and biological characterization of a novel *Schitoviridae* phage infecting *Vibrio alginolyticus*

Sofiah Tajuddin[1] · Asif M. Khan[2,3] · Li Chuin Chong[2] · Chuan Loo Wong[1] · Jia Sen Tan[1] · Md Yasin Ina-Salwany[4,5] · Han Yih Lau[6] · Kok Lian Ho[7] · Abdul Razak Mariatulqabtiah[8,9] · Wen Siang Tan[1,9]

Received: 9 June 2022 / Revised: 20 November 2022 / Accepted: 24 November 2022 / Published online: 15 December 2022

Abstract

Vibrio alginolyticus is a Gram-negative bacterium commonly associated with mackerel poisoning. A bacteriophage that specifically targets and lyses this bacterium could be employed as a biocontrol agent for treating the bacterial infection or improving the shelf-life of mackerel products. However, only a few well-characterized *V. alginolyticus* phages have been reported in the literature. In this study, a novel lytic phage, named ΦImVa-1, specifically infecting *V. alginolyticus* strain ATCC 17749, was isolated from Indian mackerel. The phage has a short latent period of 15 min and a burst size of approximately 66 particles per infected bacterium. ΦImVa-1 remained stable for 2 h at a wide temperature (27–75 °C) and within a pH range of 5 to 10. Transmission electron microscopy revealed that ΦImVa-1 has an icosahedral head of approximately 60 nm in diameter with a short tail, resembling those in the *Schitoviridae* family. High throughput sequencing and bioinformatics analysis elucidated that ΦImVa-1 has a linear dsDNA genome of 77,479 base pairs (bp), with a G + C content of ~ 38.72% and 110 predicted gene coding regions (106 open reading frames and four tRNAs). The genome contains an extremely large *virion-associated RNA polymerase* gene and two smaller *non-virion-associated RNA polymerase* genes, which are hallmarks of schitoviruses. No antibiotic genes were found in the ΦImVa-1 genome. This is the first paper describing the biological properties, morphology, and the complete genome of a *V. alginolyticus*-infecting schitovirus. When raw mackerel fish flesh slices were treated with ΦImVa-1, the pathogen loads reduced significantly, demonstrating the potential of the phage as a biocontrol agent for *V. alginolyticus* strain ATCC 17749 in the food.

Key points

- *A novel schitovirus infecting Vibrio alginolyticus ATCC 17749 was isolated from Indian mackerel.*
- *The complete genome of the phage was determined, analyzed, and compared with other phages.*
- *The phage is heat stable making it a potential biocontrol agent in extreme environments.*

Keywords *Vibrio alginolyticus* · Bacteriophage · Genome · *Schitoviridae* · Bioinformatics · Food poisoning · Biocontrol · Vibriosis

Introduction

Vibrios are Gram-negative curved-rod shape bacteria widely inhabiting aquatic environments, with many species highly pathogenic to aquatic organisms (Thompson et al. 2004). Amongst the species, *Vibrio alginolyticus* is of global concern, infecting fish (Arias et al. 1995), shrimp (Austin et al. 2003), shellfish (Panicker et al. 2004), sea cucumbers, and seahorses (Balcázar et al. 2010). Thus, vibriosis caused by *V. alginolyticus* has huge economic impacts on fisheries and aquaculture industries. Notably, this bacterium can also infect humans, leading to peritonitis (Taylor et al. 1981), intracranial infection (Opal and Saxon 1986), osteomyelitis (Barbarossa et al. 2002), otitis media (Feingold and Kumar 2004), and ocular infections (Li et al. 2009). Many cases of food poisoning in humans have been reported upon consuming seafoods contaminated with *V. alginolyticus* (Ji 1989; Smolikova et al. 2001; Xie et al. 2005). This poses menace to global food safety and public health.

✉ Asif M. Khan
makhan@bezmialem.edu.tr

✉ Wen Siang Tan
wstan@upm.edu.my

Extended author information available on the last page of the article

In the late 1950s and early 1960s, food poisoning cases due to consumption of mackerel were frequently reported in many localities along the Pacific coast of Japan (Miyamoto et al. 1961). The causative agent, *V. alginolyticus* strain ATCC 17749, was isolated from a spoiled horse mackerel by Nakamura on 7 August 1959 (Hugh and Sakazaki 1975). This strain is now widely used as a reference in studies involving *V. alginolyticus*, and its complete genome of 5,146,637 base pairs (bp) has been determined by Liu et al. (2015). Tetrodotoxin, a neurotoxin produced by *V. alginolyticus* ATCC 17749, has been demonstrated to kill mice when injected intraperitoneally (Simidu et al. 1987).

Mackerel is commonly found in tropical and temperate seas around the world (Collette et al. 2001). The fish is rich in omega-3 fatty acids and is intensively sought after by humans as food (Tridge 2020). The worldwide production of mackerel reached 5 million metric tons in 2018 (Tridge 2020). However, the flesh of mackerel spoils easily if the fish is not stored and processed immediately (Goulas and Kontominas 2005; Hardy and Smith 1976), causing food poisoning as a result. *V. alginolyticus* ATCC 17749, which causes food poisoning, is commonly isolated from mackerel (Liu et al. 2015; Molitoris et al. 1985). Thus, it is of interest to isolate a phage that infects this strain specifically. Such a specific phage could be applied as an agent of biopreservation or biocontrol targeting *V. alginolyticus* ATCC 17749, either to extend the shelf-life of mackerel products or as a treatment of vibriosis in humans caused by the strain, during which the phage is expected to cause minimal disturbance to the normal microbiota.

Before a phage can be applied as a biocontrol agent, a complete characterization of its genome and biological activities is of utmost importance to analyze the presence of antibiotic resistance genes, as well as the mode of host lysis. In the National Center for Biotechnology Information (NCBI) Genome database, as of 26 May 2022, only one schitovirus (accession: MZ447858.1), one podovirus (NC_023605.1), two inoviruses (MN719123.1, MN690600.1), and six myoviruses (NC_048747.1, NC_042100.1, NC_048779.1, NC_055862.1, NC_028829.1, NC_049477.1) infecting *V. alginolyticus* have been reported. In this study, we report the biological and genomic characterizations of a novel lytic phage, named ΦImVa-1, resembling members of the family *Schitoviridae*. This phage was isolated from Indian mackerel obtained from a local wet market in Malaysia, with *V. alginolyticus* strain ATCC 17749 as the phage host.

Materials and methods

Bacterial host and culture conditions

V. alginolyticus strain ATCC 17749 (Sakazaki 1968) was obtained from the Faculty of Agriculture, Universiti Putra Malaysia. The bacterium was grown in Luria–Bertani (LB) broth [1% (w/v) tryptone, 0.5% (w/v) yeast extract, 0.4 M NaCl and 10 mM $CaCl_2$, pH 7.5] at 35 °C with agitation at 180 rpm. Thiosulfate citrate bile sucrose (TCBS) agar (Difco, MI, USA) was used to culture the *Vibrio* sp.

Bacteriophage isolation

The fish samples, Indian mackerel, collected from a local wet market in Selangor, Malaysia, were homogenized with SM buffer [100 mM NaCl, 10 mM $MgSO_4$, 50 mM Tris–HCl (pH 7.5), and 0.01% (w/v) gelatin] and enriched with mid-log phase culture of *V. alginolyticus* for 18 h at 35 °C with agitation. The enriched sample was centrifuged at 3000 × g for 15 min, and the supernatant was filtered using a syringe filter (0.2 µm; Sartorius, Göttingen, Germany). The phage, named ΦImVa-1, was then isolated using the agar overlay assay (Adams 1959), in which equal volume of mid-log phase host culture and filtrate were added to molten agar [0.6% (w/v); 3 ml], vortexed and spread uniformly onto the surface of solid LB agar [1.5% (w/v)]. The solidified agar was then incubated for 8 h at 35 °C. Agar overlay assay was repeated for at least three times to obtain a homogenous plaque formation. The phage ΦImVa-1 is available from the corresponding author upon request.

Preparation of high titer bacteriophage suspension and purification of bacteriophage

An isolated plaque was picked and inoculated into a mid-log phase of *V. alginolyticus* culture (5 ml) and incubated at 35 °C, 180 rpm until cell lysis was observed. The mixture was centrifuged, filtered, and further used for high titer phage amplification. The filtrate was added to a mid-log phase *V. alginolyticus* culture (50 ml) at the multiplicity of infection (MOI) 0.1, and incubated at 35 °C with gentle agitation until lysis was observed. The mixture was then centrifuged at 7000 × g for 15 min at 4 °C, and the supernatant was filtered using a syringe filter (0.2 µm). The high titer phage lysate was subsequently precipitated with polyethylene glycol (PEG) 8000 [10% (w/v); Amresco, Solon, USA] and purified using cesium chloride (CsCl) density gradient ultracentrifugation for 1 h at 209,700 × g, at 4 °C. The titer of ΦImVa-1 was determined with an agar overlay assay (Chang et al. 2013).

Transmission electron microscopy

A drop of phage suspension with a titer of ~ 10^{12} pfu/ml was placed on a carbon-coated copper grid, and negatively stained with uranyl-acetate [2% (w/v), pH 4.0]. The grid was then observed under a transmission electron microscope (Hitachi H-9500, Hitachi High Technologies America, Inc., Schaumburg, IL, USA).

Examination of phage host range

The host range of ΦImVa-1 was determined using the spot test as described in Kutter and Sulakvelidze (2004), in which 200 µl of mid-log phase bacterial culture ($OD_{600} = 0.6$, and ~ 10^8 cfu/ml) was prepared as an overlay to a plate containing a bottom layer of solid LB agar, and 10 µl phage suspension (~ 10^7 pfu/ml) was aliquoted on top of the overlay agar. The agar plate was incubated at 35 °C for 8 h and examined for spot formation. Host sensitivity to the phage was determined by analyzing the lytic capabilities of the phage which formed a clear lytic spot on the plate.

Optimal multiplicity of infection

The optimal ratio of infection between ΦImVa-1 and *V. alginolyticus* strain ATCC 17749 was determined by inoculating the log phase bacterial culture with different dilutions of phage suspensions to give multiplicities of infection of 0.01, 0.1, 1, 10, and 100. Phage-free suspensions were used as controls in the experiment. The population of bacteria was enumerated at every 1-h intervals for 8 h, in which each suspension was serially diluted in a solution containing peptone [0.1% (w/v)] and NaCl [0.5% (w/v)], after that aliquots (0.1 ml) were plated onto LB agar plates. The plates were incubated at 37 °C for 18 h. All assays were performed in triplicate.

Phage adsorption and one-step growth curve

The mid-log phase culture of *V. alginolyticus* was mixed with ΦImVa-1 at MOI of 0.1. Aliquots of the suspension (100 µl) were collected every 2 min and transferred to microfuge tubes containing chloroform [2% (v/v)], vortexed and centrifuged at 12,000 × g, 4 °C, for 5 min. The supernatant was then used for the determination of unadsorbed phage titer using the agar overlay assay. The one-step growth curve was also performed to determine the latency period and burst size of the isolated phage. The mixture of phage suspension and mid-log phase culture at MOI of 0.1 was incubated for 10 min at room temperature to allow phage attachment. The mixture was then diluted 25 times in LB medium and incubated at 35 °C. Aliquots (1 ml) of the culture were taken at indicated intervals at every 5 min for 50 min consecutively, and the phage titer in the clarified samples was then determined by the double-layer assay (Wong et al. 2014).

Effects of temperature and pH on the phage-host interaction

The pelleted mid-log phase bacterial culture (~ 10^8 cfu/ml) was resuspended in LB broth (10 ml) at pH 7, and infected with the phage suspension (~ 10^7 pfu/ml; 10 ml) at MOI of 0.1. The mixture was incubated at different temperatures (27, 37, 45, 55, 65, 75, 85, and 100 °C) with agitation at 180 rpm. Initial concentrations of phage and bacteria at 0 min were determined. Phage-free suspension was used as a control along the experiment and incubated under the same conditions as the phage-bacteria mixture suspension. The adsorption assay was conducted to determine the unadsorbed phage titer according to the maximum adsorption rate based on the result of the one-step kinetic growth curve. Concurrently, the phage-bacteria suspension was continued incubating for 2 h until the bacteria lysed. Bacteria titer at 2 h was used to determine the reduction of host bacteria from phage-free and phage-bacteria suspensions.

The effect of different pH conditions on the phage-host interactions was determined using the above mentioned method with some modifications, in which the pelleted mid-log phase culture was resuspended in LB broth (MOI 0.1) of different pH values ranging from 2 to 12 and incubated at 35 °C with agitation at 180 rpm (Wong et al. 2014). In the present study, the phage was considered stable when its titer reduced by 2 $\log_{10}$. This quantitative standard was used in several studies reported previously (Merabishvili et al. 2013; Sofy et al. 2021; Wen et al. 2022; Yazdi et al. 2018; Zhang et al. 2021).

Extraction of phage nucleic acid

The nucleic acid of the purified ΦImVa-1 was extracted using the phenol chloroform method as described in Wong et al. (2014). The nucleic acid in the aqueous layer was precipitated with sodium acetate [3 M, pH 5.2; 25% (v/v)] and absolute ethanol (2 volumes). Following the centrifugation at 12,000 × g for 10 min at 4 °C, the pellet was washed twice with ethanol [70% (v/v)]. The air-dried pellet was then resuspended in TE buffer [10 mM Tris–HCl (pH 8.0) and 1 mM EDTA; 50 µl]. The quality and concentration of nucleic acid were determined with a NanoDrop spectrophotometer (Thermo Fisher Scientific, Wilmington, DE, USA).

Pulsed field gel electrophoresis and whole genome sequencing

Pulsed field gel electrophoresis (PFGE) was used to estimate the genome size of ΦImVa-1 as described in Herschleb et al. (2007). PFGE plugs were prepared, and the gel was electrophoresed at 6.0 V/cm for 20 h at 14 °C, with an initial switch at 5 s and a final switch at 60 s. The whole genome sequencing of ΦImVa-1 was performed using Illumina HiSeq (Apical Scientific, Malaysia), with a paired-ends approach of 2 × 150 bp. Paired end Illumina sequences were first removed of sequence adapters, and the reads with low quality score and/or poor quality bases were trimmed using BBduk of the BBTools Packages (https://jgi.doe.gov/data-and-tools/

bbtools) (Bushnell et al. 2017). Reads were then assembled *de novo* using the Spades genome assembler v.3.11 (https://cab.spbu.ru/software/spades/) (Bankevich et al. 2012). The quality assessment of the assembled ΦImVa-1 genome was determined by use of QUAST (http://quast.sourceforge.net/) (Gurevich et al. 2013). Filtered raw reads were also analyzed with PhageTerm (https://galaxy.pasteur.fr/) (Garneau et al. 2017) to determine the phage termini and the possible packaging mechanism. All tools were used in their default settings, except for BBduk and Spades, which were customized for the data.

Sequence analysis

Putative genes of ΦImVa-1 were determined and selected by use of RASTtk in phage mode, through the PATRIC website (https://rast.nmpdr.org/) (Brettin et al. 2015), GATU (https://4virology.net/virology-ca-tools/gatu/) (Tcherepanov et al. 2006), and Vgas (http://guolab.whu.edu.cn/vgas/) (Zhang et al. 2019). The results were both manually verified and further improved in Clone Manager 10 (Sci-Ed) software (https://www.scied.com/dl_cm10.htm). Functional inferences for candidate gene products were obtained through searches conducted using various tools: protein BLAST (http://blast.ncbi.nlm.nih.gov) (Johnson et al. 2008), Pfam (http://pfam.xfam.org) (Sonnhammer et al. 1997), InterProScan (https://www.ebi.ac.uk/interpro/) (Apweiler et al. 2001), and HHpred (https://toolkit.tuebingen.mpg.de/#/tools/hhpred) (Söding et al. 2005) server, which utilized the built-in HHpred tools against a variety of database choices offered, namely PDB_mmCIF70_11_Oct, SCOPe70_2.07, COG_KOG_v.1.0, Prosite, and NCBI_Conserved_Domains (CD)_v3.16.

Given that the tools RASTtk, Vgas, and GATU were used to predict the genes within the phage proteome, and in order to consolidate the results, those of RASTtk were used as the base for the annotation. If there was a disagreement between RASTtk and the other two tools (GATU and Vgas), the functional details of the annotations were studied from the literature/database, and if they were related, then a general description common across the tools was used. Those that were labeled as hypothetical (or simply phage protein) by RASTtk, but were annotated with a function by the other two, precedence was given to the functional curation. The gene prediction was complemented with additional functional annotation for the genes using BLASTp (*e*-value threshold of 0.05), HHpred (best hits with *e*-value of ≤ 0.05), Pfam (*e*-value threshold of 0.05), and InterPro, where applicable. Hypothetical proteins with a significant hit from any of these tools with functional information were tagged as part of the gene annotation, in the format "hypothetical: < function > ."

Screening for antibiotic resistance genes was performed by use of ABRicate (available at https://usegalaxy.eu/; https://github.com/tseemann/abricate) (Jia et al. 2017) against the Comprehensive Antibiotic Resistance Database (CARD) (Alcock et al. 2020). Additionally, the phage was screened for cleavage sites of reported restriction enzymes using the BLAST service on the REBASE web-server (http://rebase.neb.com/rebase) (Roberts et al. 2015), with selection criteria: alignment score of ≥ 40, *e*-value of ≤ 0.05, and percentage identity of $\ge 30\%$ (above the twilight zone). The molecular weight of the predicted ORFs was estimated using the batch protein molecular weight determination function of the Sequence Manipulation Suite (SMS2; http://www.bioinformatics.org/sms2/protein_mw.html) (Stothard 2000). The presence of *transfer RNA* (*tRNA*) genes was investigated by use of tRNAscan-SE (http://lowelab.ucsc.edu/tRNAscan-SE/) (Lowe and Eddy 1996) and ARAGORN (http://www.ansikte.se/ARAGORN/) (Laslett and Canback 2004).

Comparative genomics

Linear genomic comparison maps of ΦImVa-1 against closest homologs, BUCT194 (MZ447858.1) and pVco-5 (NC_055717.1), were created with pairwise tBLASTx (thresholds: *e*-value of 1×10^{-10} and a minimum of 50 amino acids alignment length) between ΦImVa-1 and BUCT194, and between ΦImVa-1 and pVco-5, to determine all possible, significant ORF (protein) homologs. These were then shortlisted by cross-checking with Expasy's (https://www.expasy.org/) (Gasteiger et al. 2003) Translate tool, whereby only ORFs exhibiting a start codon were selected, even if it was preceding the aligned match region and that the start codon may not be the first residue of the ORF. The shortlisted homologs were then visualized with EasyFig 2.2.5 (https://mjsull.github.io/Easyfig/) (Sullivan et al. 2011). The whole genome sequence (DNA) comparison of phages in NCBI Entrez Nucleotide (nt) database against ΦImVa-1 was visualized with Circoletto (http://tools.bat.infspire.org/circoletto/) (Darzentas 2010) for BLASTn matches with *e*-value selection threshold of 1×10^{-10}.

Phylogenetic trees were constructed based on the amino acid sequence of the major capsid protein, portal protein, terminase large subunit, and DNA polymerase of ΦImVa-1 compared against other prophages of the family *Schitoviridae* available in protein (nr) database, identified via a BLASTp search (default parameters, except maximum target sequence set to 250). Hits were selected for species that exhibited a significant match (*e*-value less than 0.05) to all the four query proteins. All such hits were downloaded as "FASTA (complete sequence)."

Tree generation and visualizations were performed by use of the Molecular Evolutionary Genetic Analysis (MEGA) software version 7.0, with the neighbor-joining method as the tree construction algorithm, and the robustness of the trees was assessed through bootstrapping (1000) (Kumar et al. 2016). MUSCLE (https://www.drive5.com/muscle/) (Edgar 2021) was used for multiple sequence alignment of each protein, which were manually inspected for any misalignment using BioEdit (https://bioedit.software.informer.com/7.2/) (Hall et al. 2011), and corrected where applicable. All tools were used in their default settings, unless otherwise stated such as for EasyFig and Circoletto.

Accession number

The complete nucleotide sequence of the ΦImVa-1 genome was deposited to NCBI GenBank (accession no: ON042477).

Measuring Inactivation of *V. alginolyticus* strain ATCC 17749 in raw mackerel fish flesh slices using ΦImVa-1

A raw mackerel fish was purchased from a local supermarket in Serdang, Malaysia. The fish was then aseptically cut into small slices of equal weight (2 g) and rinsed with 5 ml of SM buffer for 3 times, and sanitized by exposure to germicidal UV lamp for 10 min. *V. alginolyticus* strain ATCC 17749 (2×10^5 cfu) was spread on the fish slices, and dried for 10 min in a laminar flow hood. The fish slices without addition of any bacteria were used as a negative control. ΦImVa-1 (2×10^4 pfu in SM buffer) was then dropped on the contaminated fish slices to achieve an MOI of 0.1. SM buffer (100 µl) was added to the contaminated fish slices as a positive control. The samples were incubated at room temperature (25 °C) for 2, 3, and 4 h. The samples were then homogenized in 5 ml of high salt lysogeny broth [1% (w/v) tryptone, 0.5% (w/v) yeast extract, 0.4 M NaCl, 10 mM $CaCl_2$] using pellet pestles. Homogenized mackerel samples (100 µl) were plated on TCBS agar, and incubated overnight at 37 °C for enumeration of viable *V. alginolyticus*.

Statistical analysis

Statistical analysis was performed by use of the IBM SPSS statistics software version 23 (IBM, Armonk, NY, USA). The effects of pH and temperatures on phage-host interaction, variations in the adsorption rate and reduction of *Vibrio* titer at different pH and temperatures, as well as inactivation of *Vibrio* using ΦImVa-1 as a biocontrol agent were analyzed with the one-way analysis of variance (ANOVA). Significant differences in the experiments were determined using the Duncan's multiple-range tests, in which *p* values of < 0.01 were considered as significant.

Results

Plaque and virion morphologies

ΦImVa-1, isolated from Indian mackerel, produced clear and round plaques of approximately 1–2 mm in diameter (Fig. 1a) with *V. alginolyticus* strain ATCC 17749 as its host. Transmission electron microscopic analysis of negatively stained ΦImVa-1 revealed an icosahedral head with a diameter of approximately 60 nm and a short tail (Fig. 1b). The tail structure is similar in appearance with that of bacteriophage vB_VspP_pVa5, a N4-like lytic bacteriophage infecting *Vibrio splendidus* (Katharios et al. 2017), which was proposed to be grouped in the family of *Schitoviridae* (Wittmann et al. 2020). Generally, the morphology of ΦImVa-1 resembles that of bacteriophages in the family *Schitoviridae* (Walker et al. 2021; Wittmann et al. 2020).

Phage host range

Phage lysis test was carried out using the spot test on several different *Vibrio* species and strains to determine the host range of ΦImVa-1 (Table 1). Out of the 26 different *Vibrio* species and strains tested, ΦImVa-1 exhibited a narrow host spectrum, and only specifically infected *V. alginolyticus* strain ATCC 17749, and none of the other species and strains was lysed.

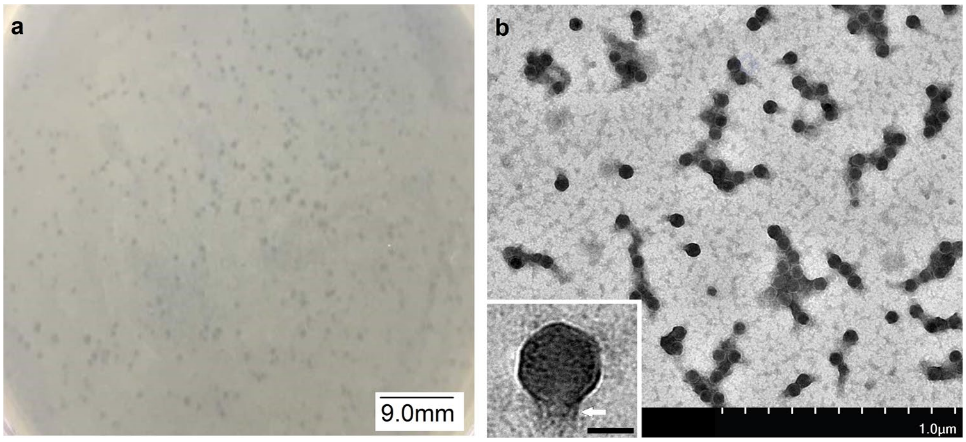

Fig. 1 Plaque and virion morphologies of ΦImVa-1. (**a**) Plaque morphology of ΦImVa-1 with *V. alginolyticus* strain ATCC 17749 on Luria–Bertani (LB) double-layer agar plate after incubating at 35 °C for 8 h. (**b**) Transmission electron micrograph of negatively stained ΦImVa-1 virions with 2% (w/v) uranyl acetate. Inset at the bottom shows the enlarged ΦImVa-1 morphology with a black scale bar (50 nm). The white arrow indicates the short tail

Table 1 Host range determination of ΦImVa-1

Species	Strain	Reference	Host range
Vibrio alginolyticus	ATCC 17749	Sakazaki 1968	+
Vibrio alginolyticus	PKGL12	MN253146.1	–
Vibrio alginolyticus	PKL13	MN253173.1	–
Vibrio alginolyticus	PKGS29	MN253155.1	–
Vibrio alginolyticus	PKS12	MN253171.1	–
Vibrio alginolyticus	PKGK21	MN253152.1	–
Vibrio alginolyticus	PKS15	MN253176.1	–
Vibrio alginolyticus	NK26	MN253204.1	–
Vibrio alginolyticus	PKGL15	MN253150.1	–
Vibrio alginolyticus	PKK15	MN253177.1	–
Vibrio parahaemolyticus	ATCC 17802	CP014046.2	–
Vibrio parahaemolyticus	PB1937	CP022243.1	–
Vibrio parahaemolyticus	PKK14	MN253384.1	–
Vibrio parahaemolyticus	PKK24	MN253388.1	–
Vibrio communis	PKL18	MN253305.1	–
Vibrio communis	NS14	MN253310.1	–
Vibrio communis	NL30	MN253318.1	–
Vibrio communis	NS28	MN253317.1	–
Vibrio harveyi	NCIMB1280	NR_043165.1	–
Vibrio harveyi	PJK21	MN253329.1	–
Vibrio harveyi	PJS28	MN253330.1	–
Vibrio vulnificus	NL15	MN253453.1	–
Vibrio vulnificus	PJS19	MN253428.1	–
Vibrio tubiashii	PJK19	MN253418.1	–
Vibrio anguillarium	ATCC 43313	X71817.1	–
Vibrio mytili	LS23	MN253340.1	–

(+) Bacteria were lysed; (−) bacteria were not lysed

Optimization of MOI

The optimal MOI ratio of ΦImVa-1 was 0.1, in which the host was reduced by 4.40 log$_{10}$ cfu/ml at 8-h incubation (Fig. 2). Conversely, MOI ratio of 1 had the lowest reduction of host by only 1.61 log$_{10}$ cfu/ml at 8-h incubation. At higher MOI ratios of 10 and 100, the host only reduced by 1.89 and 2.80 log$_{10}$ cfu/ml, respectively, at 8-h incubation.

Burst size, latent period, and phage adsorption rate

The time required for 95% of ΦImVa-1 to adsorb and infect the host, *V. alginolyticus* strain ATCC 17749, was approximately 12 min (Fig. 3a). From the one-step growth curve of ΦImVa-1, the latent period was approximately 15 min with an average burst size of 66 virions per cell at MOI of 0.1 (Fig. 3b).

Effect of pH and temperature on phage-host interaction

The ΦImVa-1 phage was stable within pH 5–10, in which the titer of free phage after incubation for 2 h was within 2 log$_{10}$pfu/ml as compared with the initial phage titer (Fig. 4a). However, at pH 3–4 and pH 11, the phage titer reduced significantly. The phage was inactivated at pH 2 and 12. Figure 4b shows that ΦImVa-1 was stable at 27, 37, 45, 55, 65, and 75 °C, in which a reduction of less than 1 log$_{10}$ pfu/ml was observed after 2 h of incubation. However, the phage titer reduced dramatically at 85 °C with 2.91 log$_{10}$ cfu/ml and inactivated at 100 °C.

The adsorption rate of ΦImVa-1 varied at different pH range, in which the phage displayed high adsorption rate at pH 7–9 (Fig. 5a). However, its adsorption rate was significantly affected at pH 3–6 and pH 10–11. The highest reduction of the *Vibrio* host cell by ΦImVa-1 was at pH 7 with approximately 7.29 log$_{10}$ cfu/ml.

In general, ΦImVa-1 adsorbed well to *V. alginolyticus* strain ATCC 17749 at 27 °C, 37 °C, and 45 °C with an adsorption rate of ~ 75.17%, ~ 81.71%, and ~ 75.95%, respectively (Fig. 5b). However, at higher temperatures, the adsorption rate reduced significantly to ~ 69.83%, ~ 68.43%, and ~ 57.15% at 55 °C, 65 °C, and 75 °C, respectively.

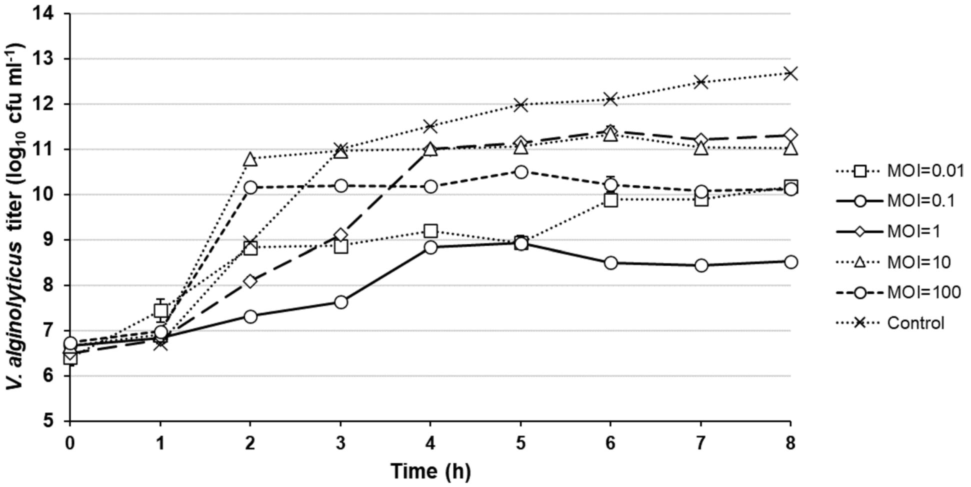

Fig. 2 Inactivation of *Vibrio alginolyticus* strain ATCC 17749 by ΦImVa-1 at different MOI ratios. The titers of the bacteria were determined after being infected with ΦImVa-1 at different interval time periods. The bacteria culture in the absence of the phage was used as a control. Error bars represent the standard deviations of three replicates of plate counts per MOI

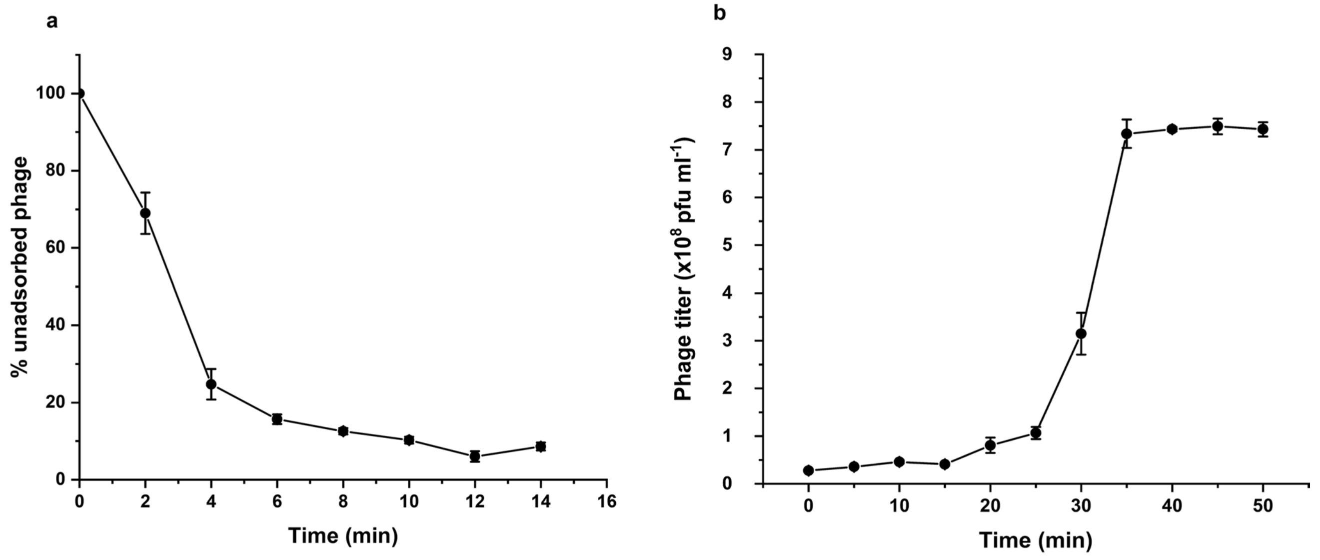

Fig. 3 Biological characterization of phage ΦImVa-1. (**a**) The adsorption rate of ΦImVa-1 to *V. alginolyticus* strain ATCC 17749 was assessed at every 2-min interval for 14 min consecutively at 35 °C, at an MOI of 0.1. (**b**) A one-step growth curve of ΦImVa-1 with *V. alginolyticus* strain ATCC 17749 as its host. Error bars represent the standard deviations of three independent experiments

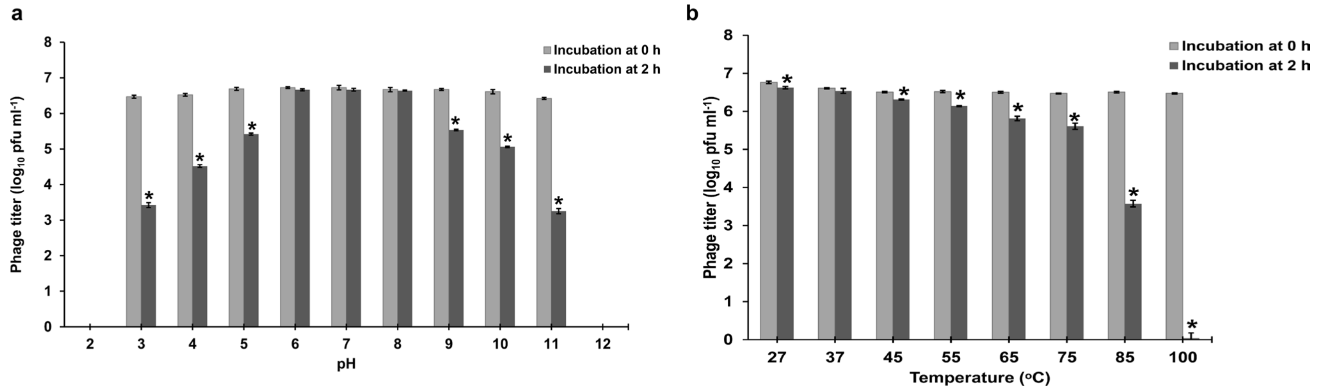

Fig. 4 Thermal and pH stability of ΦImVa-1. The phage was incubated at different pHs (**a**) and temperatures (**b**) for 2 h, and its survivability was determined using the agar overlay assay. Error bars represent the standard deviations of three independent experiments. * represents significant difference ($p < 0.01$) between the phage titer incubated at 0 h and 2 h

Enumeration of *Vibrio* host cell titer revealed that ΦImVa-1 reduced the highest amount of *Vibrio* host cell at 37 °C and 45 °C, with reduction rates of 8.44 $\log_{10}$ cfu/ml and 8.01 $\log_{10}$ cfu/ml, respectively. However, ΦImVa-1 showed the lowest reduction rate of host bacteria at 27 °C, which was approximately 3.42 $\log_{10}$ cfu/ml.

Genome size estimation and whole genome sequencing of ΦImVa-1

The genome size of ΦImVa-1 was approximately 75 kbp as analyzed using PFGE (Fig. 6). Whole genome sequencing revealed that ΦImVa-1 comprised of 77,479 bp with a G + C content of ~ 38.66%. The genome's termini and the possible packaging mechanisms were predicted according to the *in silico* determination method, PhageTerm (Garneau et al. 2017), which predicted that ΦImVa-1 has a linear dsDNA with short direct terminal repeats of 569 bases.

Characteristics of the *Vibrio* phage ΦImVa-1 genome

The genome of ΦImVa-1 harbors 110 candidate predicted gene regions (106 ORFs plus four putative *tRNA* genes), 20 of which were leftward-directed, and 90 were rightward-directed (Table 2). Of these, 19 were determined to

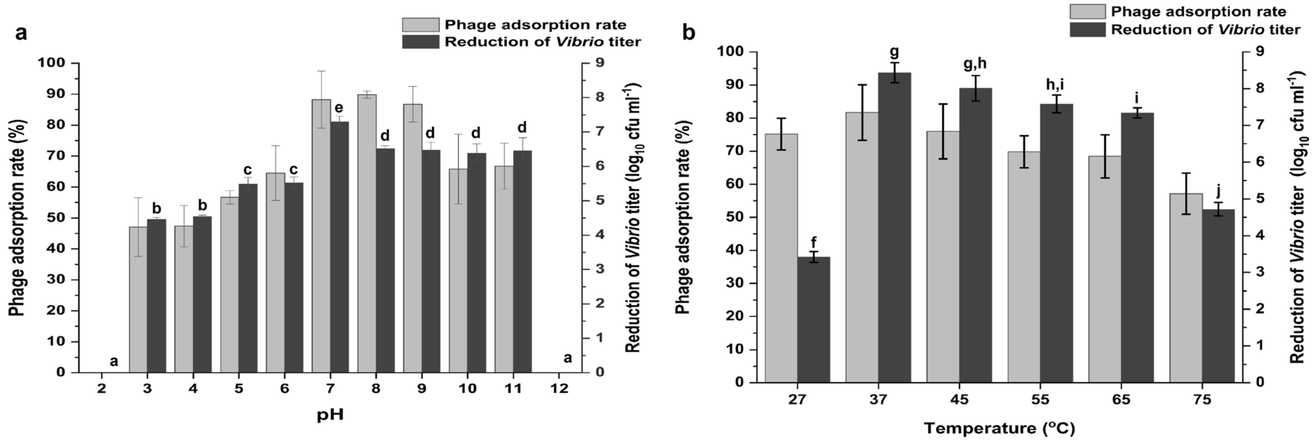

Fig. 5 The adsorption rate of ΦImVa-1 onto *V. alginolyticus* strain ATCC 17749 and the reduction of its host cell at different pHs (**a**) and temperatures (**b**). Error bars represent the standard deviations of three independent experiments. The values which are marked by different letters are significantly different ($p < 0.01$)

have a predicted (putative) function, and 91 were classified as hypothetical proteins. The genes with a predicted function were clustered into seven functional categories: virion structural and assembly proteins (5), viral protein synthesis (4), DNA transcription (3), nucleotide metabolism (3), DNA replication (2), cell lysis (1), and others (1) (Fig. 7). The majority (91) of the genes were predicted as hypothetical proteins and merit further investigation of their functional role(s). Nonetheless, possible function was annotated for 15, whereby an inference could be made from a search across functional databases (InterPro/Pfam/HHpred/BLASTp).

In the phage genome, as many as four putative *tRNA* genes, which are categorized herein under “viral protein synthesis” (Fig. 7), were identified by RASTk for three of the amino acids, named proline (Pro-TGT), asparagine (Asn-GTT), and arginine (Arg-TCT), and a tRNA suppressor (Sup-TTA). Except for tRNA-Sup-TTA, the three *tRNA* genes for the amino acids were in congruence with the tools ARAGON and tRNAscan-SE. Separately, screening against the CARD database indicated that the genome does not encode gene products associated with antibiotic resistance. The phage was evaluated for its involvement in the restriction modification system (RM). None of the computationally annotated ORFs indicated methyltransferase or endonuclease function. As for the restriction enzyme cleavage sites, the database showed that *V. alginolyticus* strain ATCC 17749 coded for three type I and two type II RM system enzymes. However, only the cleavage site for type I putative N6-adenine DNA methyltransferase was provided (recognition site: GATC), which was observed at various locations in the phage genome.

Comparative genomic analyses

Similarity search of the full genome of ΦImVa-1 with nucleotide BLAST (blastn instead of megablast and low complexity regions filter turned off) returned the best match to *Vibrio* phage BUCT194 with a high sequence similarity and high length coverage (~ 85.09% sequence identity and ~ 88% query coverage); the earliest noted date for BUCT194 in the database record was 21 June 2021. The second-best match was to *Vibrio* phage pVco-5 with a high sequence similarity (~ 71.57% identity), but low query coverage (~ 23%). Of the 106 predicted ORFs of ΦImVa-1, 94 were similar to 92 ORFs of BUCT194, with a few of the former aligned to the same ORFs of the latter (Supplementary Table S4). In contrast, only 30 of the ΦImVa-1 ORFs were similar to pVco-5, aligning to 32 ORFs (Supplementary Table S5). Of the 19 ORFs with putative functions, 10 (ORF 82, virion-encapsulated RNA polymerase; ORF 70, DNA polymerase; ORF 72, phosphoribosyl-ATP pyrophosphohydrolase; ORF 76, AAA domain protein; ORF 59, membrane protein TerC; ORF 88, major capsid protein; ORF 91, portal protein; ORF 95, long tail fiber distal subunit; ORF 97, terminase large subunit; and ORF 68, metallopeptidase domain protein) were common to both ΦImVa-1 and BUCT194 genomes (Fig. 7). Similarly, nine of the putative ORFs were common between ΦImVa-1 and pVco-5 genomes, where six (ORF 70, ORF 76, ORF 82, ORF 88, ORF 91, and ORF 97) were also shared with BUCT194 and three were different (ORFs 27 and 28, DNA-directed RNA polymerase; and ORF 38, N-acetylmuramoyl-L-alanine amidase).

The genome of ΦImVa-1 phage was further compared with those of the four most closely related *Vibrio* phages

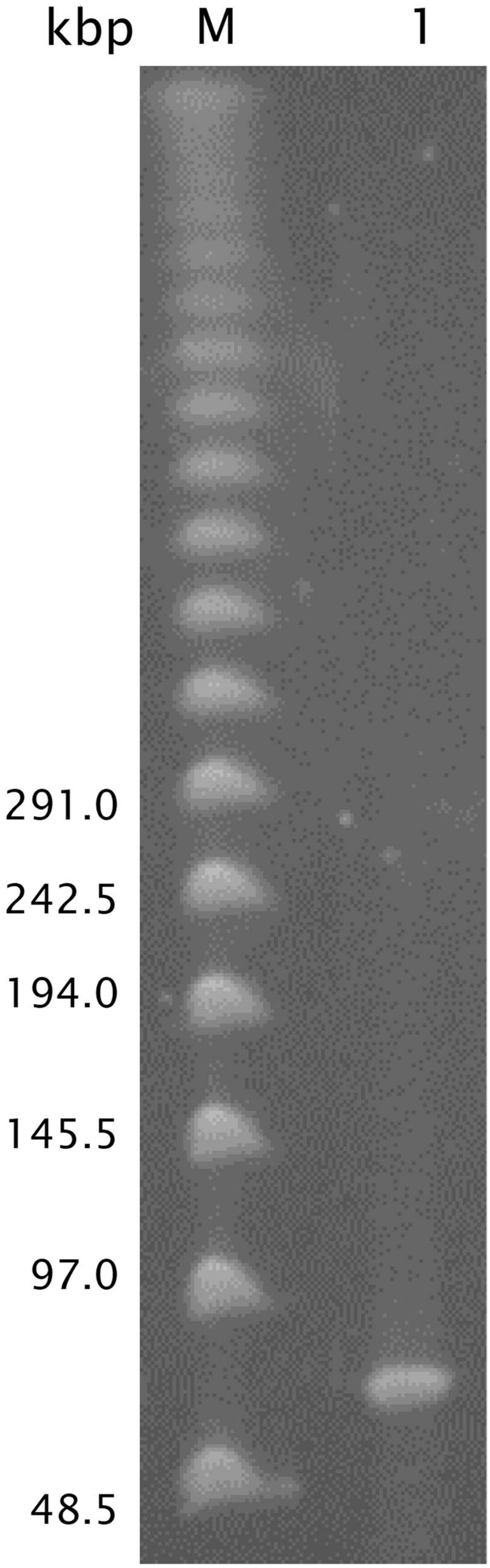

Fig. 6 Pulsed field gel electrophoresis (PFGE) of ΦImVa-1 genome. Lane M: lambda-ladder PFG marker. Lane 1: ΦImVa-1

(identified through BLASTn against Nucleotide database; sequence identity > 72%) (Fig. 8). Both ΦImVa-1 (coordinates: 73,596–73,752) and BUCT194 (54,048–54,207) genomes shared sequence identity (~ 84% and ~ 87%) only to a limited region of phi50-12 (GenBank MN584918.1) that was 156 bp (coordinates: 2227–2071) and 159 bp long (coordinates: 2227–2068), respectively. The phi50-12 showed no discernible DNA sequence similarity to phage pVco-5 and phi 1 (GenBank NC_028799.1). However, phi 1 showed sequence similarity to ΦImVa-1 with ten sequence homolog regions. Therefore, the genome of ΦImVa-1 is highly similar to the recently deposited BUCT194, and both differ significantly at the nucleotide level from the previously reported *Vibrio* phage pVco-5 genome. Phylogenetic analysis of ΦImVa-1 protein sequences (DNA polymerase, Fig. 9; major capsid protein, Supplementary Fig. S1; portal protein, Supplementary Fig. S2; and terminase large subunit, Supplementary Fig. S3) with homologs from other reported members of the *Caudovirales* order (including BUCT194) revealed that ΦImVa-1 was closely related to BUCT194, followed by pVco-5 (Fig. 9, Fig. S1-Fig. S3). Although BUCT194 has been classified as a member of *Schitoviridae* in NCBI, no information is available on its biological properties and morphology in the literature. As for pVco-5, it is a schitovirus infecting *Vibrio coralliilyticus*.

Inactivation of *V. alginolyticus* strain ATCC 17749 in raw mackerel fish flesh slices using ΦImVa-1

The feasibility of ΦImVa-1 as a biocontrol agent for *V. alginolyticus* strain ATCC 17749 in raw mackerel fish flesh was examined. The bacteria were spiked on the surface of fish flesh slices, and the phage at an MOI of 0.1 was applied to the contaminated fish slices as this is the optimal MOI ratio of the phage to the bacterium. When the fish slices were left at room temperature (25 °C) without the addition of ΦImVa-1, 1013 and 1817 cfu/g ($p < 0.01$) of bacteria were detected at 3 and 4 h, respectively (Fig. 10). When the fish slices were treated with ΦImVa-1, the pathogen loads reduced dramatically to 213 and 450 cfu/g ($p < 0.01$) at 3 and 4 h, respectively, demonstrating the potential of ΦImVa-1 as a biocontrol agent for *V. alginolyticus* strain ATCC 17749 in raw mackerel fish.

Discussion

In this study, we have isolated and characterized the complete genome of the phage ΦImVa-1, which exhibits a narrow host range and specific lytic activity against *V. alginolyticus* ATCC 17749. Transmission electron microcopy revealed that ΦImVa-1 is related to *Schitoviridae* family with an icosahedral head and a short tail. The classification of ΦImVa-1 in this family was further supported by the results of comparative genomic analyses using the complete genome sequence of the phage. Host range analysis using 26 *Vibrio* species showed that ΦImVa-1 has a very narrow host spectrum, infecting only *V. alginolyticus* strain ATCC 17749, which was used as a host for isolation of the phage. Other *Vibrio* phages with a very narrow host range have also been reported previously, such as VpVs (Comeau et al. 2006), VEN (Kokkari et al. 2018), ΦH2, ΦH8, ΦH20, ΦS4-7, ΦS4-18, and Φ2E-1 (Tan et al. 2014). The narrow host range is attributed to specific interactions between a phage receptor binding protein (RBP) with a single receptor present on a host cell during the initial stage of phage infection (Abdelsattar et al. 2021). The optimal MOI ratio of ΦImVa-1 to *V. alginolyticus* strain ATCC 17749 was 0.1, and the host did not develop resistance against the phage within the experimental period (8 h).

The ΦImVa-1 phage adsorbed rapidly to its host in approximately 12 min, indicating an efficient binding of the phage to host receptors. Thereafter, the phage propagated rapidly in the host with a latent period of 15 min and a burst size of 66 particles per cell. The latent period and burst size of phage ΦImVa-1 are significantly shorter and smaller than those of other *V. alginolyticus* phages: BUCT549 (30–40 min, 141 pfu/cell; Li et al. 2021a), vB_ValP_IME234 (60 min, 390 pfu/cell; Li et al. 2021b), and Vp670 (30 min, 84 pfu/cell; Luo et al. 2018). A shorter latent period is normally associated with a smaller burst size because a shorter time period is used for the synthesis of phage nucleic acids and proteins, as well as the assembly of phage progenies before lysis of a host (Shao and Wang 2008). The ΦImVa-1 remained active with variations within 1.55 $\log_{10}$ pfu/ml after being incubated for 2 h at 35 °C from pH 5 to 10 and stayed stable even at 75 °C.

The ΦImVa-1 has a linear dsDNA genome of 77,479 bp, including short direct terminal repeats of 569 bases. These genomic features are consistent with phages in *Schitoviridae* family, comprising of a genome ranging from 59 to 80 kb and including terminal repeats (Wittmann et al. 2020). The genome does not encode gene products associated with antibiotic resistance as per the screening of the CARD database. Further, none of the phage ORFs was predicted to exhibit methyltransferase or endonuclease activity. Additionally, only one RM system enzyme cleavage site for type I putative N6-adenine DNA methyltransferase was observed in the phage genome. Restriction endonuclease and methyltransferase are part of the RM system, which protects the host genome against foreign DNA (Enikeeva et al. 2010). The absence or limited number of cleavage sites in a phage genome offers the phage advantage in terms of evading the restriction enzyme systems of the host bacteria, thereby potentially increasing not only the survival ability, but also the chance to infect other bacteria. Little is known on the specific role of adenine methyltransferase (DAM), whether expressed in the host or the phage, in the life cycle regulation of bacteriophages (Bochow et al. 2012).

The hallmark of schitoviruses is the presence of an extremely *large virion-associated RNA polymerase* (vRNAP) gene, along with two smaller *non-virion-associated RNA polymerase* (nvRNAP) genes (Wittmann et al. 2020). As for ΦImVa-1, ORFs 27 and 28 potentially encode nvRNAPs, which show high similarity with the hypothetical proteins of BUCT194 (GenBank acc. no. UAW01195.1, ~ 94.17% sequence identity; GenBank acc. no. UAW01197.1, ~ 98.55% sequence identity, respectively). The largest ORF of ΦImVa-1 (ORF 82) potentially encodes vRNAP, which shared high similarity with homologs from BUCT194 (GenBank acc. no. UAW01149.1, ~ 82.44% sequence similarity) and pVco-5 (GenBank acc. no. YP_010089972.1, ~ 37.39% sequence similarity). Schitovirus vRNAP is introduced into the bacteria at the beginning of infection for the transcription of early genes (Falco et al. 1980; Rothman-Denes and Schito 1974). Consequently, the viral middle and late genes are transcribed by the two nvRNAPs (Carter et al. 2003; Willis et al. 2002). The ΦImVa-1 ORF25 hypothetically encodes a ssDNA-binding RNA polymerase cofactor (Drc), similar to that of *Pseudomonas* phage LUZ7 (6QLC_A, based on HHpred database, ~ 99.55% probability in percent). Drc is suggested to interact with unwound single-stranded promoters and recruit the phage RNA polymerase for transcriptions (Boon et al. 2020).

The ΦImVa-1 is a lytic phage; thus, it should express lysis proteins that disrupt the bacterial cell wall comprising of peptidoglycan and membrane. ORF 38 encodes a putative endolysin N-acetylmuramoyl-L-alanine amidase (MurNAc-LAA; InterPro: IPR002508; Pfam: PF01520.18; HHpred: cd02696; ~ 98.45% probability), which showed high similarity with alanyl-tRNA synthetase encoded by BUCT194 (GenBank acc. No. UAW01210.1, ~ 96.57% sequence identity). ORF 46 encodes a hypothetical outer membrane murein-binding lipoprotein Lpp (HHpred: COG4238; ~ 97.1% probability). The presence of this ORF in ΦImVa-1 genome is peculiar given the bacterial origin of Lpp, with no homolog in any other viruses. Separately, its location in ΦImVa-1 genome, within the lysis cassette, possibly suggests that it could affect the efficiency or timing of the host lysis during the release of phage progenies. Additionally, ORF 48 encodes a hypothetical spanin (HHpred: P39503; ~ 97.36% probability), which is equivalent to phage lambda Rz/Rz1-like protein, disrupting the host outer membrane during cell lysis (Summer et al. 2007).

The ΦImVa-1 ORF 59 potentially codes for an integral membrane protein, TerC (BLASTp, HHpred, and InterPro), involved in tellurite resistance (Burian et al. 1998). This ORF shared high similarity with TerC family metal homeostasis membrane protein of BUCT194 (GenBank acc. no UAW01125.1, ~93.81% sequence identity). A cluster of *Ter* genes that confers tellurite resistance has been discovered in many pathogenic bacteria, including *Escherichia coli* O157:H7, *Staphylococcus aureus*, and *Vibrio cholerae* (Donovan and van Netten 1995; Zadik et al. 1993). In this present

Table 2 Genes predicted within the *Vibrio* phage ΦImVa-1 genome. The molecular weight of each ORF, predicted by use of SMS2, is provided in Table S1

Gene	Start	Stop	Strand	Gene annotation
ORF 1	120	320	+	Hypothetical protein
ORF 2	470	655	+	Hypothetical protein
ORF 3	793	936	+	Hypothetical protein
ORF 4	923	1045	+	Hypothetical protein
ORF 5	1509	1850	+	Hypothetical protein
ORF 6	2275	2448	+	Hypothetical protein
ORF 7	2445	2609	+	Hypothetical protein
ORF 8	2597	2797	+	Hypothetical protein
ORF 9	2785	3024	+	Hypothetical protein
ORF10	3171	3389	+	Hypothetical protein
ORF 11	3376	3588	+	Hypothetical protein
ORF 12	3585	3794	+	Hypothetical protein
ORF 13	3799	4578	+	Hypothetical protein
ORF 14	4777	4950	+	Hypothetical protein
ORF 15	4947	5144	+	Hypothetical protein
ORF 16	5206	5358	+	Hypothetical protein
ORF 17	5345	5551	+	Hypothetical protein
ORF 18	5541	5663	+	Hypothetical protein
ORF 19	5665	5877	+	Hypothetical: plasmid maintenance system killer protein
ORF 20	5887	6000	+	Hypothetical protein
ORF 21	6140	6343	+	Hypothetical protein
ORF 22	6334	6543	+	Hypothetical protein
ORF 23	6702	6875	+	Hypothetical protein
ORF 24	6875	7105	+	Hypothetical protein
ORF 25	7232	7507	+	Hypothetical: ssDNA binding RNA polymerase cofactor
ORF 26	7575	7916	+	Hypothetical protein
ORF 27	7967	9256	+	DNA-directed RNA polymerase
ORF 28	9301	10,548	+	DNA-directed RNA polymerase
ORF 29	10,600	10,794	+	Hypothetical protein
ORF 30	10,952	11,092	+	Hypothetical protein
ORF 31	11,168	11,371	+	Hypothetical protein
ORF 32	11,447	11,728	+	Hypothetical protein
ORF 33	11,719	11,904	+	Hypothetical protein
ORF 34	12,033	12,278	+	Hypothetical protein
ORF 35	12,413	12,598	+	Hypothetical protein
ORF 36	12,665	12,877	+	Hypothetical protein
ORF 37	12,855	13,211	+	Hypothetical protein
ORF 38	13,738	13,208	−	N-acetylmuramoyl-L-alanine amidase
ORF 39	13,760	14,068	+	Hypothetical protein
ORF 40	14,068	14,553	+	Hypothetical protein
ORF 41	14,944	15,156	+	Hypothetical protein
ORF 42	15,437	15,586	+	Hypothetical protein
ORF 43	15,658	15,864	+	Hypothetical protein
ORF 44	15,979	16,776	+	Hypothetical protein
ORF 45	16,826	17,026	+	Hypothetical protein
ORF 46	17,031	17,729	+	Hypothetical: outer membrane murein-binding lipoprotein
ORF 47	17,738	18,031	+	Hypothetical protein
ORF 48	18,079	18,363	+	Hypothetical: spanin
ORF 49	18,356	18,511	+	Hypothetical protein
ORF 50	18,508	18,801	+	Hypothetical protein
ORF 51	18,804	18,995	+	Hypothetical protein
tRNA-1	19,052	19,125	+	tRNA-Pro-TGG
tRNA-2	19,134	19,205	+	tRNA-Asn-GTT
tRNA-3	19,307	19,380	+	tRNA-Arg-TCT
ORF 52	19,407	20,039	+	Hypothetical protein
tRNA-4	20,388	20,502	+	tRNA-Sup-TTA

Table 2 (continued)

Gene	Start	Stop	Strand	Gene annotation
ORF 53	20,640	22,079	+	Hypothetical protein
ORF 54	22,347	22,925	+	Hypothetical: dihydrofolate reductases
ORF 55	22,922	23,518	+	Hypothetical protein
ORF 56	24,220	24,882	+	Hypothetical: TerD domain protein
ORF 57	24,930	25,610	+	Hypothetical: TerD domain protein
ORF 58	25,610	26,029	+	Hypothetical: TerB family protein
ORF 59	26,062	27,081	+	Integral membrane protein TerC
ORF 60	27,186	27,611	+	Hypothetical: TerB family protein
ORF 61	27,611	27,865	+	Hypothetical protein
ORF 62	27,881	28,075	+	Hypothetical protein
ORF 63	28,075	28,398	+	Hypothetical: SaV protein
ORF 64	28,398	28,562	+	Hypothetical protein
ORF 65	28,572	29,264	+	Hypothetical protein
ORF 66	34,126	29,363	−	Hypothetical: L-shaped tail fiber protein p132
ORF 67	34,286	35,449	+	ATPase
ORF 68	35,500	36,732	+	Metallopeptidase domain protein
ORF 69	36,775	37,215	+	Hypothetical protein
ORF 70	37,215	40,025	+	DNA polymerase
ORF 71	40,124	40,315	+	Hypothetical protein
ORF 72	40,385	40,843	+	Phosphoribosyl-ATP pyrophosphohydrolase
ORF 73	40,830	41,831	+	Hypothetical: RecB family exonuclease
ORF 74	41,842	44,001	+	Hypothetical: DNA replication licensing factor; primase C terminal 1
ORF 75	44,005	44,220	+	Hypothetical protein
ORF 76	44,220	44,954	+	AAA domain protein
ORF 77	45,034	45,750	+	ssDNA binding protein
ORF 78	45,757	45,948	+	Hypothetical protein
ORF 79	45,938	46,063	+	Hypothetical protein
ORF 80	46,094	46,483	+	Hypothetical: endodeoxyribonuclease RusA
ORF 81	46,480	47,223	+	Hypothetical protein
ORF 82	56,442	47,254	−	Virion-encapsulated RNA polymerase
ORF 83	57,749	56,451	−	Hypothetical protein
ORF 84	58,158	57,760	−	Hypothetical protein
ORF 85	60,329	58,155	−	Hypothetical protein
ORF 86	61,482	60,391	−	Hypothetical protein
ORF 87	61,984	61,487	−	Hypothetical protein
ORF 88	63,352	62,036	−	Major capsid protein
ORF 89	64,524	63,370	−	Hypothetical protein
ORF 90	64,884	64,528	−	Hypothetical protein
ORF 91	66,991	64,877	−	Portal protein
ORF 92	67,266	67,030	−	Hypothetical protein
ORF 93	67,580	67,263	−	Hypothetical protein
ORF 94	68,170	67,649	−	Hypothetical protein
ORF 95	72,137	68,157	−	Long tail fiber distal subunit
ORF 96	72,820	72,134	−	Hypothetical protein
ORF 97	74,415	72,823	−	Terminase large subunit
ORF 98	74,671	74,402	−	Hypothetical protein
ORF 99	75,348	74,671	−	Hypothetical: terminase small subunit
ORF 100	75,400	75,588	+	Hypothetical protein
ORF 101	75,683	75,865	+	Hypothetical protein
ORF 102	75,862	76,062	+	Hypothetical protein
ORF 103	76,212	76,397	+	Hypothetical protein
ORF 104	76,535	76,678	+	Hypothetical protein
ORF 105	76,665	76,787	+	Hypothetical protein
ORF 106	77,251	77,382	+	Hypothetical protein

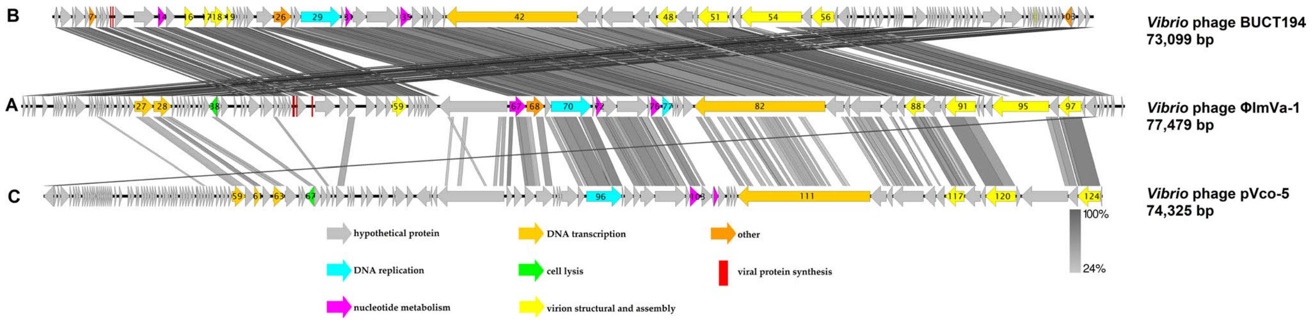

Fig. 7 Genome organizations and location of homologous proteins of (**A**) ΦImVa-1, (**B**) BUCT194 (Table S2), and (**C**) pVco-5 (Table S3) phages. Arrows indicate transcriptional orientation of genes; while rectangles indicate orientation of tRNAs. Selected predicted (putative and hypothetical) protein functions are indicated by colored arrows according to the legend. The numbers on the arrows refer to locus tags, i.e., ORF XXX, where X refer to gene numbers in Table 2. The lines connecting phage sequence arrows reflect protein sequence similarity according to the scale. The genes located in the genomes of ΦImVa-1, BUCT194, and pVco-5 are provided in Supplementary Tables S1, S2, and S3, respectively

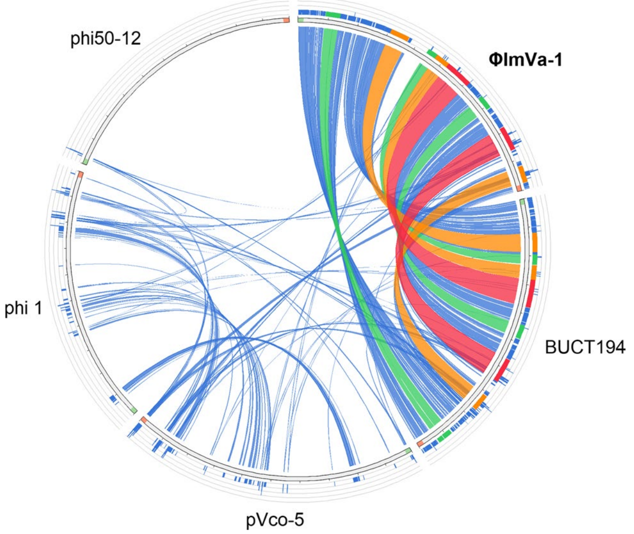

Fig. 8 Comparison of *Vibrio* phage ΦImVa-1 with other *Vibrio* phages. Similarities were based on all against all nucleotide BLAST search. Similarities are reflected by the ribbons connecting ideograms. Their colors reflect the scale of similarities between phage genome part; the color signifies "score/max" ratio with blue ≤ 0.25, green ≤ 0.50, orange ≤ 0.75, and red > 0.75. Green and orange rectangles at the ends of the ideogram reflect the beginning and end of the phage genome, respectively

study, ΦImVa-1 hypothetical *Ter* genes are clustered from ORFs 56 to 60: TerD domain proteins (ORFs 56 and 57) and TerB family proteins (ORFs 58 and 60). The ORFs 56 and 57 show high similarities to TerD domain proteins of BUCT194 (GenBank acc. no. UAW01123.1, ~ 99.09% sequence identity) and *Chitinophaga eiseniae* (GenBank acc. no. WP_078671465.1, ~ 35.71% sequence identity), respectively. The ORFs 58 and 60 shared high similarity with TerB family proteins of BUCT194 (GenBank acc. no UAW01124.1, ~ 94.24% sequence identity; GenBank acc. no. UAW01126.1, ~ 97.16% sequence identity, respectively).

Generally, the packaging and assembly machineries of tailed dsDNA phages consist of terminase, portal, capsid, and tail fiber proteins. After the viral DNA replication, the resulting concatemeric DNA is digested into genome-sized lengths by the terminase and subsequently packaged into the preassembled capsid using the ATPase. The terminase contains two subunits: terminase large (TerL) and terminase small (TerS) subunits (Yang et al. 2017). A predicted ΦImVa-1 TerL (ORF 97) shared high similarity with homologs from BUCT194 (GenBank acc. no. UAW01163.1, ~ 97.92% sequence identity) and pVco-5 phage (GenBank acc. no. YP_010089985.1, ~ 74.91% sequence identity). The ΦImVa-1 TerS is hypothetically encoded by ORF 99 (HHpred: 6W7T_B; ~ 96.82% probability), which is closely located to ORF 97, encoding TerL. The icosahedral head of schitoviruses is made up of capsid proteins that protect the viral DNA from outer environment. The ΦImVa-1 ORF 88 potentially codes for a major capsid protein, which has a significant degree of similarity to homologs from BUCT194 (GenBank acc. no. UAW01155.1, ~ 96.35% sequence identity), pVco-5 (GenBank acc. no. YP_010089978.1, 63.49% sequence identity), and Enterobacteria phage N4 (HHpred: Q859Q5, ~ 97.81% probability). Portal proteins play important roles in DNA packaging and ejection of tailed phages (Prevelige and Cortines 2018). The ΦImVa-1 ORF 91 codes for a putative portal protein, which shared ~ 94.60% and ~ 64.02% sequence identity with homologs from BUCT194 (GenBank acc. no. UAW01158.1) and pVco-5 (GenBank acc. no. YP_010089981.1), respectively. The short tail component of schitoviruses recognizes and adsorbs on cell surface receptors and injects DNA into the host (Maffei et al. 2021). The ΦImVa-1 ORF 66 hypothetically encodes a tail fiber protein sharing high similarity with L-shaped tail fiber protein p132 (HHpred: Q7Y5D9, ~ 97.11% probability) of

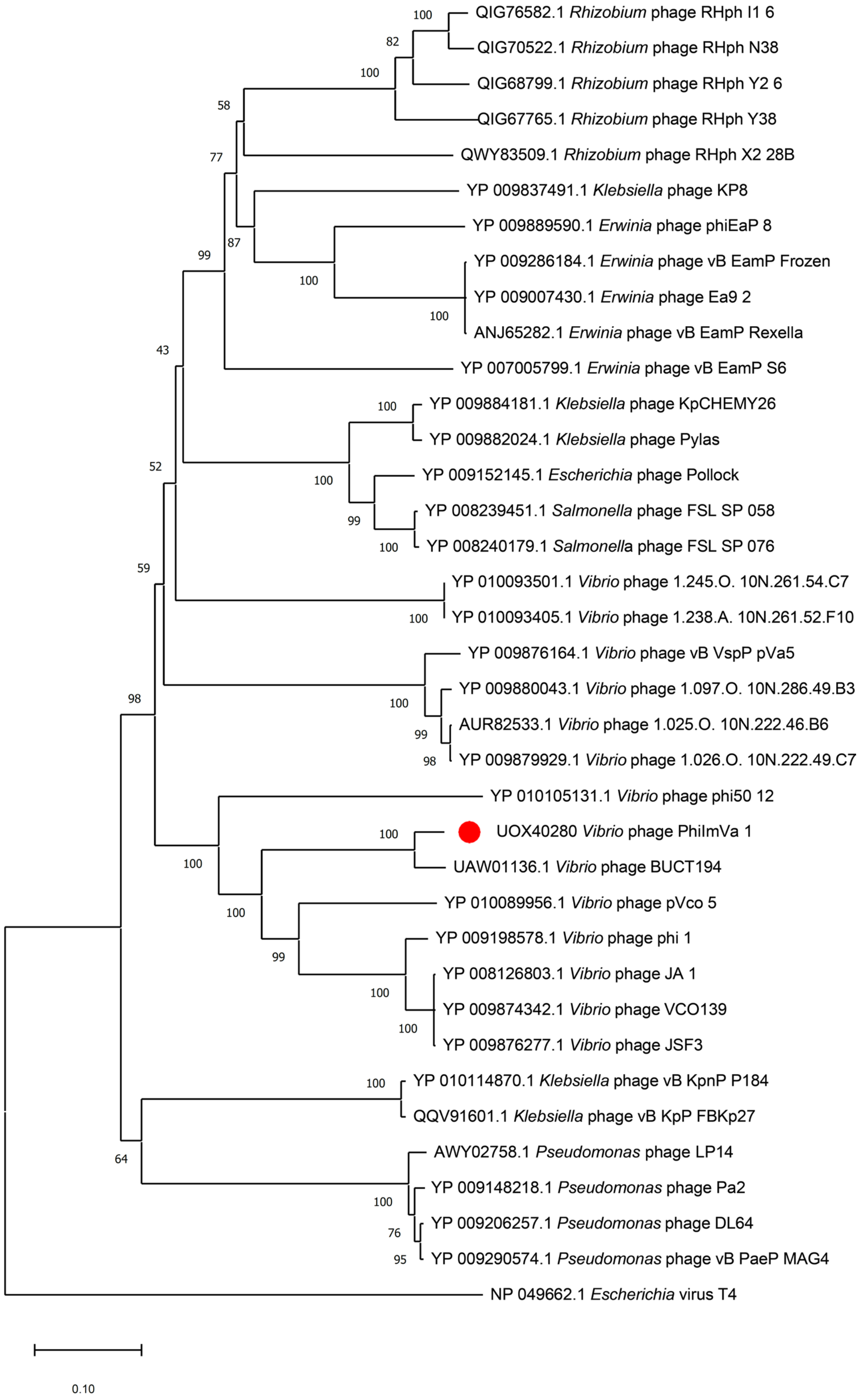

Fig. 9 A phylogram constructed using the DNA polymerase protein of *Vibrio* phage ΦImVa-1, which was compared to corresponding proteins of other prophages available in NCBI Protein database. The other prophages were of the family *Schitoviridae*, identified via a BLASTp search (default parameters, except maximum target sequence set to 250). Hits were selected for species that also exhibited a significant match (*e*-value less than 0.05) to the other three proteins analyzed (major capsid protein, portal protein, and large terminase subunit protein). The tool MEGA7 was used to generate the tree, utilizing neighbor-joining method, with 1000 bootstrap replicates. The *Escherichia* virus T4 protein from subfamily Tevenvirinae was used as an outgroup to root the tree

Enterobacteria phage T5 (Zivanovic et al. 2014). The gene encoding for the putative long tail fiber distal subunit (ORF 95) shared ~ 83.20% sequence identity with a homolog from BUCT194 (GenBank acc. no. UAW01161.1). The C-terminal end of this subunit contains a chaperone of endosialidase domain (InterPro: IPR030392; Pfam: PF13884), which

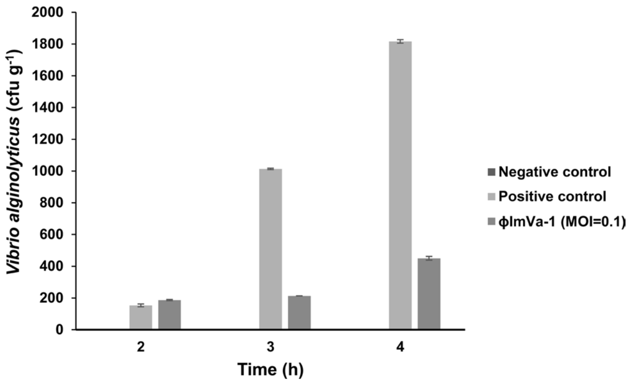

Fig. 10 ΦImVa-1 as a biocontrol agent of *V. alginolyticus* strain ATCC 17749 in raw mackerel fish flesh slices. *V. alginolyticus* strain ATCC 17749 was spread on mackerel fish flesh slices. The fish slices without addition of any bacteria were used as a negative control. ΦImVa-1 was then dropped on the contaminated fish slices to achieve an MOI of 0.1. SM buffer was added to the contaminated fish slices as a positive control. The samples were incubated at room temperature (25 °C) for 2, 3, and 4 h. The samples were then homogenized, plated on TCBS agar, and incubated overnight at 37 °C for enumeration of viable *V. alginolyticus*. Error bars represent the standard deviations of three independent experiments

degrades poly α2,8-sialic acid of encapsulated pathogenic bacteria during the phage infection process (Stummeyer et al. 2005).

In relation to nucleotide metabolism functions, ΦImVa-1 potentially encodes three putative ATPase/AAA proteins: ATPase (ORF 67; InterPro: IPR027417; Pfam: PF12775), phosphoribosyl-ATP pyrophosphohydrolase (ORF 72), and AAA domain protein (ORF 76), as well as a dihydrofolate reductase (ORF 54), based on BLAST/InterPro/Pfam matches. The putative ATPase (DNA dependent) exhibits a significant sequence similarity with several hypothetical proteins from different *Vibrio* phages, such as BUCT194 (UAW01132.1: ~ 98.97% similarity), phi 1 (YP_009198571.1: ~ 57.33% similarity), JA-1 (YP_008126798.1: ~ 58.92% similarity), JSF3 (YP_009876285.1: ~ 59.51% similarity), pVco-5 (YP_010089949.1: ~ 57.85% similarity), and phi50-12 (YP_010105139.1: ~ 40.16% similarity). The ORF 67 is predicted to belong to the P-loop containing nucleoside triphosphate hydrolase superfamily (InterPro: IPR027417), having AAA_7 and CbbQ/NirQ/NorQ domains, which are known to be involved in ATP-dependent protein packaging/binding mechanisms. Such AAA ATPase enzymes (P-loop NTPase superfamily) have been reported to be molecular motors, which catalyze the packaging of the viral genome in an energy-dependent manner (Kedzierska 2006; Leipe et al. 2003). The putative phosphoribosyl-ATP pyrophosphohydrolase (InterPro: IPR021130; Pfam: PF01503.17) encoded by ORF 72 potentially catalyzes the second step in the histidine biosynthesis pathway. The protein exhibits ~ 94.74% sequence identity with a homolog from BUCT194 (GenBank acc. no. UAW01138.1). The ΦImVa-1 ORF 76 is postulated to belong to the AAA + superfamily, with a AAA_24 (OF13479) Rossmann fold p-loop containing alpha/beta structure (HHpred: best hit; PDB 1C9K_A, ~ 91.89% probability). The protein has ~ 97.95% sequence identity with the AAA domain protein of BUCT194 (GenBank acc. no. UAW01142.1). The ΦImVa-1 ORF 54 hypothetically encodes dihydrofolate reductase (InterPro: IPR012259; Pfam: PF00186), the key enzyme in folate metabolism, with ~ 92.71% sequence identity to dihydrofolate reductase of BUCT194 (GenBank acc. no. UAW01121.1). This enzyme catalyzes the NADPH-dependent reduction of dihydrofolate to tetrahydrofolate, which can be used for *de novo* synthesis of certain amino acids and for DNA precursor synthesis (Trimble et al. 1988).

Concerning viral replication, ORF 70 potentially encodes a DNA polymerase (InterPro: IPR002298; Pfam: PF00476.20; HHpred: COG0749, ~ 93.79% probability), which shared ~ 96.26% and ~ 60.54% sequence identity with homologs from BUCT194 (GenBank acc. no UAW01136.1) and pVco-5 (GenBank acc. no. YP_010089956.1), respectively. Two potential domains are detected within the gene: DNA-directed DNA polymerase, family A, palm domain (InterPro: IPR001098) and 3′–5′ exonuclease domain (InterPro: IPR002562), which catalyze the accurate replication of DNA and the hydrolysis of unpaired or mismatched nucleotides, respectively (Jung et al. 1987; Lehman 2003). This gene is also associated with 3 other superfamilies: DNA/RNA polymerase superfamily (InterPro: IPR043502), ribonuclease H-like superfamily (InterPro: IPR12337), and ribonuclease H superfamily (InterPro: IPR036397). The ΦImVa-1 ORF 77 potentially encodes the single-stranded DNA binding (SSB) protein, which acts as an architectural transcription factor by providing an active promoter confirmation for vRNAP binding (Cho et al. 1995). The putative ORF 77 SSB protein shared ~ 88.70% and ~ 40.49% sequence identity, respectively, with homologs from BUCT194 (GenBank acc. no. UAW01143.1) and JA-1 (GenBank acc. no. YP_008126814.1), which play a role in DNA repair and reorganization, and activate the DNA polymerase and helicase. Sequence comparison showed that ORF 73 encodes a hypothetical RecB exodeoxyribonuclease V exonuclease (InterPro: IPR011604; HHpred: COG2887, ~ 99.2% probability), potentially classified as a member of the phage-type exonucleases superfamily, consisting of a common core fold at the C-terminus that is closely related in sequence and structure with a homolog in the phage lambda (Kovall and Matthews 1997). The exonuclease of phage lambda facilitates DNA recombination through a double-strand break repair and single-strand annealing pathways; it is also important for the late, rolling-circle mode of the viral DNA replication. The ORF 74 hypothetically encodes a protein that is similar to the DNA replication licensing factor protein, also known as putative minichromosome maintenance complex component 7 (MCM7) (HHpred: 6RAW_7, 98.65% probability), which forms a heterohexameric ring that hydrolyzes ATP and provides the motor function for DNA unwinding complex (Iyer et al. 2005). MCM as a DNA helicase is found in both eukaryotes and archaea (Ausiannikava and Allers 2017; Bochman and Schwacha 2009). It is suggested to serve as a host factor that regulates viral genome replication (Kawaguchi and Nagata 2007), and several phages have been reported to possess an *MCM-like* gene (Bochman and Schwacha 2009). The C-terminal end of the protein contains a primase C terminal 1 (Pfam: PF08708) of alpha helical domain (655–717 aa) (Iyer et al. 2005). It is likely that ORF 80 encodes a hypothetical Holliday junction resolvase RusA-like endodeoxyribonuclease (InterPro: IPR008822; HHpred: COG4570, ~ 90.98% probability), which is involved in ΦImVa-1 replication. The RusA protein of *E. coli* is a DNA endonuclease that can resolve Holliday intermediates and correct the defect in genetic recombination and DNA repair during DNA replication (Macmaster et al. 2006).

The ΦImVa-1 genome harbors four putative *tRNA* genes involved in viral protein synthesis: *tRNA-Pro-TGT*, *tRNA-Asn-GTT*, *tRNA-Arg-TCT*, and *tRNA-suppressor-TTA*. Bailly-Bechet et al. (2007) indicate that tRNAs present in phage genomes are those that are rare in hosts, which allow the phages to gain an absolute advantage over their competitors by producing their proteins more efficiently. The tRNA-suppressor-TTA can recognize a stop codon, and instead of termination, it inserts an amino acid at the position in the polypeptide chain. In phages, suppressor tRNAs have been shown to alleviate nonsense mutations, which facilitate restoration of normal phenotypes, albeit altered by an amino acid substitution (Gesteland et al. 1967; Model et al. 1969). Whether the tRNA-suppressor-TTA of ΦImVa-1 serves a similar or different purpose, it requires further investigation.

In conclusion, this study has provided insights into the biological and genomic properties of the phage ΦImVa-1, a novel schitovirus that specifically infects *V. alginolyticus* ATCC 17749. The ΦImVa-1 adsorbed rapidly to its host and lysed the cell in 15 min. Moreover, ΦImVa-1 was stable within pH 5 to 10 and demonstrated thermal stability up to 75 °C, enabling its use in different environments. The ΦImVa-1 significantly reduced the pathogen loads in mackerel fish flesh slices, demonstrating the potential of the phage as a biocontrol agent for *V. alginolyticus* strain ATCC 17749 in the food. Genomic analysis of ΦImVa-1 revealed diverse gene functions and their possible underlying mechanisms, which significantly contributed to our current knowledge about schitoviruses infecting *V. alginolyticus*.

Supplementary Information The online version contains supplementary material available at https://doi.org/10.1007/s00253-022-12312-3.

Author contribution ST designed and conducted the experiments, analyzed data, and wrote the manuscript. AMK conceived and designed the experiments, analyzed data, supervised the project, provided resources, reviewed and edited the manuscript. LCC and CLW analyzed data and reviewed the manuscript. JST designed and conducted the experiments. MYIS, HYL, KLH, and ARM provided resources, supervised the project, and reviewed the manuscript. WST conceived and designed the experiments, analyzed data, supervised the project, provided resources, acquired funding, reviewed and edited the manuscript. All authors read and approved the manuscript.

Funding This study was supported by UPM grant (No: UPM/800–3/3/1/GPB/2019/9682500).

Data availability All relevant data are included in this article and its supplementary materials. The nucleotide sequence of the phage genome was deposited to NCBI GenBank and is accessible through the entry record accession no: ON042477.

Declarations

Ethics approval This article does not contain any studies with human participants or animals performed by any of the authors.

Conflict of interest The authors declare no competing interests.

References

Abdelsattar AS, Dawooud A, Rezk N, Makky S, Safwat A, Richards PJ, El-Shibiny A (2021) How to train your phage: the recent efforts in phage training. Biologics 1:70–88. https://doi.org/10.3390/BIOLOGICS1020005

Adams M (1959) Bacteriophages. Wiley Interscience, New York

Alcock BP, Raphenya AR, Lau TT, Tsang KK, Bouchard M, Edalatmand A, Huynh W, Nguyen AL, Cheng AA, Liu S, Min SY (2020) CARD 2020: antibiotic resistome surveillance with the comprehensive antibiotic resistance database. Nucleic Acids Res 48:D517–D525. https://doi.org/10.1093/nar/gkz935

Apweiler R, Attwood TK, Bairoch A, Bateman A, Birney E, Biswas M, Bucher P, Cerutti L, Corpet F, Croning MDR, Durbin R, Falquet L, Fleischmann W, Gouzy J, Hermjakob H, Hulo N, Jonassen I, Kahn D, Kanapin A, Zdobnov EM (2001) The InterPro database, an integrated documentation resource for protein families, domains and functional sites. Nucleic Acids Res 29:37–40. https://doi.org/10.1093/nar/29.1.37

Arias CR, Garay E, Aznar R (1995) Nested PCR method for rapid and sensitive detection of *Vibrio vulnificus* in fish, sediments, and water. Appl Environ Microbiol 61:3476–3478. https://doi.org/10.1128/aem.61.9.3476-3478.1995

Ausiannikava D, Allers T (2017) Diversity of DNA replication in the archaea. Genes 8:1–14. https://doi.org/10.3390/genes8020056

Austin B, Pride AC, Rhodie GA (2003) Association of a bacteriophage with virulence in *Vibrio harveyi*. J Fish Dis 26:55–58. https://doi.org/10.1046/j.1365-2761.2003.00413.x

Bailly-Bechet M, Vergassola M, Rocha E (2007) Causes for the intriguing presence of tRNAs in phages. Genome Res 17:1486–1495. https://doi.org/10.1101/gr.6649807

Balcázar JL, Gallo-Bueno A, Planas M, Pintado J (2010) Isolation of *Vibrio alginolyticus* and *Vibrio splendidus* from captive-bred seahorses with disease symptoms. Antonie Van Leeuwenhoek 97:207–210. https://doi.org/10.1007/s10482-009-9398-4

Bankevich A, Nurk S, Antipov D, Gurevich AA, Dvorkin M, Kulikov AS, Lesin VM, Nikolenko SI, Pham S, Prjibelski AD, Pyshkin AV, Sirotkin AV, Vyahhi N, Tesler G, Alekseyev MA, Pevzner PA (2012) SPAdes: a new genome assembly algorithm and its applications to single-cell sequencing. J Comput Biol 19:455–477. https://doi.org/10.1089/cmb.2012.0021

Barbarossa V, Kučišec-Tepeš N, Aldova E, Matek D, Stipoljev F (2002) Ilizarov technique in the treatment of chronic osteomyelitis caused by *Vibrio alginolyticus*. Croat Med J 43:346–349

Bochman ML, Schwacha A (2009) The Mcm complex: unwinding the mechanism of a replicative helicase. Microbiol Mol Biol Rev 73:652–683. https://doi.org/10.1128/mmbr.00019-09

Bochow S, Elliman J, Owens L (2012) Bacteriophage adenine methyltransferase: a life cycle regulator? Modelled using *Vibrio harveyi* myovirus like. J Appl Microbiol 113:1001–1013. https://doi.org/10.1111/j.1365-2672.2012.05358.x

Boon M, De Zitter E, De Smet J, Wagemans J, Voet M, Pennemann FL, Schalck T, Kuznedelov K, Severinov K, Van Meervelt L, De Maeyer M (2020) "Drc", a structurally novel ssDNA-binding transcription regulator of N4-related bacterial viruses. Nucleic Acids Res 48:445–459. https://doi.org/10.1093/nar/gkz1048

Brettin T, Davis JJ, Disz T, Edwards RA, Gerdes S, Olsen GJ, Olson R, Overbeek R, Parrello B, Pusch GD, Shukla M, Thomason JA, Stevens R, Vonstein V, Wattam AR, Xia F (2015) RASTtk: a modular and extensible implementation of the RAST algorithm for building custom annotation pipelines and annotating batches of genomes. Sci Rep 5:8365. https://doi.org/10.1038/srep08365

Burian J, Tu N, Kl'učár L, Guller L, Lloyd-Jones G, Stuchlík S, Fejdi P, Siekel P, Turňa J (1998) *In vivo* and *in vitro* cloning and phenotype characterization of tellurite resistance determinant conferred by plasmid pTE53 of a clinical isolate of *Escherichia coli*. Folia Microbiol 43:589–599. https://doi.org/10.1007/BF02816374

Bushnell B, Rood J, Singer E (2017) BBMerge – accurate paired shotgun read merging via overlap. PLoS ONE 12:1–15. https://doi.org/10.1371/journal.pone.0185056

Carter RH, Demidenko AA, Hattingh-Willis S, Rothman-Denes LB (2003) Phage N4 RNA polymerase II recruitment to DNA by a single-stranded DNA-binding protein. Genes Dev 17:2334–2345. https://doi.org/10.1101/gad.1121403

Chang Y, Lee JH, Shin H, Heu S, Ryu S (2013) Characterization and complete genome sequence analysis of *Staphylococcus aureus* bacteriophage SA12. Virus Genes 47:389–393. https://doi.org/10.1007/s11262-013-0938-7

Cho NY, Choi M, Rothman-Denes LB (1995) The bacteriophage N4-coded single-stranded DNA-binding protein (N4SSB) is the transcriptional activator of *Escherichia coli* RNA polymerase at N4 late promoters. J Mol Biol 246:461–471. https://doi.org/10.1006/jmbi.1994.0098

Collette BB, Reeb C, Block BA (2001) Systematics of the tunas and mackerels (*Scombridae*). Fish Physiol 19:1–33. https://doi.org/10.1016/S1546-5098(01)19002-3

Comeau AM, Chan AM, Suttle CA (2006) Genetic richness of vibriophages isolated in a coastal environment. Environl Microbiol 8:1164–1176. https://doi.org/10.1111/j.1462-2920.2006.01006.x

Darzentas N (2010) Circoletto: visualizing sequence similarity with Circos. Bioinforma 26:2620–2621. https://doi.org/10.1093/bioinformatics/btq484

Donovan TJ, van Netten P (1995) Culture media for the isolation and enumeration of pathogenic *Vibrio* species in foods and environmental samples. Int J Food Microbiol 26:77–91. https://doi.org/10.1016/0168-1605(95)00015-c

Edgar RC (2021) MUSCLE v5 enables improved estimates of phylogenetic tree confidence by ensemble bootstrapping. BioRxiv. https://doi.org/10.1101/2021.06.20.449169

Enikeeva FN, Severinov KV, Gelfand MS (2010) Restriction–modification systems and bacteriophage invasion: who wins? J Theor Biol 266:550–559. https://doi.org/10.1016/j.jtbi.2010.07.006

Falco SC, Zehring W, Rothman-Denes LB (1980) DNA-dependent RNA polymerase from bacteriophage N4 virions. Purification and characterization. J Biol Chem 255:4339–4347. https://doi.org/10.1016/S0021-9258(19)85670-3

Feingold MH, Kumar ML (2004) Otitis media associated with *Vibrio alginolyticus* in a child with pressure-equalizing tubes. Pediatr Infect Dis J 23:475–476. https://doi.org/10.1097/01.INF.0000126592.19378.30

Garneau JR, Depardieu F, Fortier LC, Bikard D, Monot M (2017) PhageTerm: a tool for fast and accurate determination of phage termini and packaging mechanism using next-generation sequencing data. Sci Rep 7:1–10. https://doi.org/10.1038/s41598-017-07910-5

Gasteiger E, Gattiker A, Hoogland C, Ivanyi I, Appel RD, Bairoch A (2003) ExPASy: the proteomics server for in-depth protein knowledge and analysis. Nucleic Acids Res 31:3784–3788. https://doi.org/10.1093/nar/gkg563

Gesteland RF, Salser W, Bolle A (1967) *In vitro* synthesis of T4 lysozyme by suppression of amber mutations. Proc Natl Acad Sci USA 58:2036–2042. https://doi.org/10.1073/pnas.58.5.2036

Goulas AE, Kontominas MG (2005) Effect of salting and smoking-method on the keeping quality of chub mackerel (*Scomber japonicus*): biochemical and sensory attributes. Food Chem 93:511–520. https://doi.org/10.1016/j.foodchem.2004.09.040

Gurevich A, Saveliev V, Vyahhi N, Tesler G (2013) QUAST: quality assessment tool for genome assemblies. Bioinforma 29:1072–1075. https://doi.org/10.1093/bioinformatics/btt086

Hall T, Biosciences I, Carlsbad C (2011) BioEdit: an important software for molecular biology. GERF Bull Biosci 2:60–61

Hardy R, Smith JGM (1976) The storage of mackerel (*Scomber scombrus*). Development of histamine and rancidity. J Science Food and Agri 27:595–599. https://doi.org/10.1002/JSFA.2740270702

Herschleb J, Ananiev G, Schwartz DC (2007) Pulsed-field gel electrophoresis. Nat Protoc 2:677–684. https://doi.org/10.1038/nprot.2007.94

Hugh R, Sakazaki R (1975) International Committee on Systematic Bacteriology Subcommittee on the taxonomy of *vibrios*: minutes of the closed meeting, 3 September 1974. Int J Syst Bacteriol 25:389–391. https://doi.org/10.1099/00207713-25-4-389

Iyer LM, Koonin EV, Leipe DD, Aravind L (2005) Origin and evolution of the archaeo-eukaryotic primase superfamily and related palm-domain proteins: structural insights and new members. Nucleic Acids Res 33:3875–3896. https://doi.org/10.1093/nar/gki702

Ji SP (1989) The first isolation of *Vibrio alginolyticus* from samples which caused food poisoning. Zhonghua Yu Fang Yi Xue Za Zhi [Chinese Journal of Preventive Medicine] 23:71–73. https://europepmc.org/article/med/2737046

Jia B, Raphenya AR, Alcock B, Waglechner N, Guo P, Tsang KK, Lago BA, Dave BM, Pereira S, Sharma AN, Doshi S (2017) CARD 2017: expansion and model-centric curation of the comprehensive antibiotic resistance database. Nucleic Acids Res 45:D566–D573. https://doi.org/10.1093/nar/gkw1004

Johnson M, Zaretskaya I, Raytselis Y, Merezhuk Y, McGinnis S, Madden TL (2008) NCBI BLAST: a better web interface. Nucleic Acids Res 36:W5–W9. https://doi.org/10.1093/nar/gkn201

Jung GH, Leavitt MC, Hsieh JC, Ito J (1987) Bacteriophage PRD1 DNA polymerase: evolution of DNA polymerases. Proc Natl Acad Sci USA 84:8287–8291. https://doi.org/10.1073/pnas.84.23.8287

Katharios P, Kalatzis PG, Kokkari C, Sarropoulou E, Middelboe M (2017) Isolation and characterization of a N4-like lytic bacteriophage infecting *Vibrio splendidus*, a pathogen of fish and bivalves. PLoS One 12:e0190083. https://doi.org/10.1371/journal.pone.0190083

Kawaguchi A, Nagata K (2007) *De novo* replication of the influenza virus RNA genome is regulated by DNA replicative helicase, MCM. EMBO J 26:4566–4575. https://doi.org/10.1038/sj.emboj.7601881

Kedzierska S (2006) Structure, function and mechanisms of action of ATPases from the AAA superfamily of proteins. Postepy Biochemii 52:330–338. https://europepmc.org/article/med/17201069

Kokkari C, Sarropoulou E, Bastias R, Mandalakis M, Katharios P (2018) Isolation and characterization of a novel bacteriophage infecting *Vibrio alginolyticus*. Arch Microbio 200:707–718. https://doi.org/10.1007/s00203-018-1480-8

Kovall R, Matthews BW (1997) Toroidal structure of λ-exonuclease. Sci 277:1824–1827. https://doi.org/10.1126/science.277.5333.1824

Kumar S, Stecher G, Tamura K (2016) MEGA7: molecular evolutionary genetics analysis version 7.0 for bigger datasets. Mol Biol Evol 33:1870–1874. https://doi.org/10.1093/molbev/msw054

Kutter E, Sulakvelidze A (2004) Bacteriophages: biology and applications. CRC Press. https://doi.org/10.1201/9780203491751

Laslett D, Canback B (2004) ARAGORN, a program to detect tRNA genes and tmRNA genes in nucleotide sequences. Nucleic Acids Res 32:11–16. https://doi.org/10.1093/nar/gkh152

Lehman IR (2003) Discovery of DNA polymerase. J Biol Chem 278:34733–34738. https://doi.org/10.1074/jbc.X300002200

Leipe D, Koonin EV, Aravind L (2003) Evolution and classification of P-loop kinases and related proteins. J Mol Biol 333:781–815. https://doi.org/10.1016/j.jmb.2003.08.040

Li XC, Xiang ZY, Xu XM, Yan WH, Ma JM (2009) Endophthalmitis caused by *Vibrio alginolyticus*. J Clin Microbiol 47:3379–3381. https://doi.org/10.1128/JCM.00722-09

Li J, Tian F, Hu Y, Lin W, Liu Y, Zhao F, Ren H, Pan Q, Shi T, Tong Y (2021) Characterization and genomic analysis of BUCT549, a novel bacteriophage infecting *Vibrio alginolyticus* with flagella as receptor. Front Microbiol 12:668319. https://doi.org/10.3389/fmicb.2021.668319

Li F, Tian F, Li J, Li L, Qiao H, Dong Y, Ma F, Zhu S, Tong Y (2021) Isolation and characterization of a podovirus infecting the opportunist pathogen *Vibrio alginolyticus* and *Vibrio parahaemolyticus*. Virus Res 302:198481. https://doi.org/10.1016/j.virusres.2021.198481

Liu XF, Cao Y, Zhang HL, Chen YJ, Hu CJ (2015) Complete genome sequence of *Vibrio alginolyticus* ATCC 17749^T. Am Soc Microbiol 3:1500–1514. https://doi.org/10.1128/genomeA.01500-14

Lowe TM, Eddy SR (1996) TRNAscan-SE: a program for improved detection of transfer RNA genes in genomic sequence. Nucleic Acids Res 25:955–964. https://doi.org/10.1093/nar/25.5.0955

Luo P, Yun L, Li Y, Tian Y, Liu Q, Huang W, Hu C (2018) Complete genomic sequence of the *Vibrio alginolyticus* bacteriophage Vp670 and characterization of the lysis-related genes, cwlQ and holA. BMC Genomics 19:741. https://doi.org/10.1186/s12864-018-5131-x

Macmaster R, Sedelnikova S, Baker PJ, Bolt EL, Lloyd RG, Rafferty JB (2006) RusA Holliday junction resolvase: DNA complex structure - insights into selectivity and specificity. Nucleic Acids Res 34:5577–5584. https://doi.org/10.1093/nar/gkl447

Maffei E, Shaidullina A, Burkolter M, Heyer Y, Estermann F, Druelle V, Sauer P, Willi L, Michaelis S, Hilbi H, Thaler DS, Harms A (2021) Systematic exploration of *Escherichia coli* phage–host interactions with the BASEL phage collection. PLoS Biol 19:e3001424. https://doi.org/10.1371/JOURNAL.PBIO.3001424

Merabishvili M, Vervaet C, Pirnay JP, De Vos D, Verbeken G, Mast J, Chanishvili N, Vaneechoutte M (2013) Stability of *Staphylococcus aureus* phage ISP after freeze-drying (lyophilization). PLoS One 8:e68797. https://doi.org/10.1371/journal.pone.0068797

Miyamoto Y, Nakamuma K, Takizawa K (1961) Pathogenic halophiles. Proposals of a new genus "*Oceanomonas*" and of the amended species names. Jpn J Microbiol 5:477–486. https://doi.org/10.1111/j.1348-0421.1961.tb00225.x

Model P, Webster RE, Zinder ND (1969) The UGA codon *in vitro*: chain termination and suppression. J Mol Biol 43:177–190. https://doi.org/10.1016/0022-2836(69)90087-4

Molitoris E, Joseph SW, Krichevsky MI, Sindhuhardja W, Colwell RR (1985) Characterization and distribution of *Vibrio alginolyticus* and *Vibrio parahaemolyticus* isolated in Indonesia. Appl Environ Microbiol 50:1388–1394. https://doi.org/10.1128/AEM.50.6.1388-1394.1985

Opal SM, Saxon JR (1986) Intracranial infection by *Vibrio alginolyticus* following injury in salt water. J Clin Microbio 23:373–374. https://doi.org/10.1128/jcm.23.2.373-374.1986

Panicker G, Myers ML, Bej AK (2004) Rapid detection of *Vibrio vulnificus* in shellfish and gulf of Mexico water by real-time PCR. Appl Environ Microbiol 70:498–507. https://doi.org/10.1128/AEM.70.1.498-507.2004

Prevelige PE, Cortines JR (2018) Phage assembly and the special role of the portal protein. Curr Opin Virol 31:66–73. https://doi.org/10.1016/J.COVIRO.2018.09.004

Roberts RJ, Vincze T, Posfai J, Macelis D (2015) REBASE—a database for DNA restriction and modification: enzymes, genes and genomes. Nucleic Acids Res 43:D298–D299. https://doi.org/10.1093/nar/gku1046

Rothman-Denes LB, Schito GC (1974) Novel transcribing activities in N4-infected *Escherichia coli*. Virol 60:65–72. https://doi.org/10.1016/0042-6822(74)90366-3

Sakazaki R (1968) Proposal of *Vibrio alginolyticus* for the biotype 2 of *Vibrio parahaemolyticus*. Jpn J Med Sci Biol 21:359–362. https://doi.org/10.7883/YOKEN1952.21.359

Shao Y, Wang IN (2008) Bacteriophage adsorption rate and optimal lysis time. Genet 180:471–482. https://doi.org/10.1534/GENETICS.108.090100

Simidu U, Noguchi T, Hwang DF, Shida Y, Hashimoto K (1987) Marine bacteria which produce tetrodotoxin. Appl Environ Microbiol 53:1714–1715. https://doi.org/10.1128/aem.53.7.1714-1715.1987

Smolikova LM, Lomov IM, Khomenko TV, Murnachev GP, Kudriakova TA, Fetsailova OP, Sanamiants EM, Makedonova LD, Kachkina GV, Golenishcheva EN (2001) Studies on halophilic *vibrios* causing a food poisoning outbreak in the city of Vladivostok. Zhurnal Mikrobiologii, Epidemiologii i Immunobiologii 6:3-7. https://pubmed.ncbi.nlm.nih.gov/11881491/

Söding J, Biegert A, Lupas AN (2005) The HHpred interactive server for protein homology detection and structure prediction. Nucleic Acids Res 33:W244–W248. https://doi.org/10.1093/nar/gki408

Sofy AR, El-Dougdoug NK, Refaey EE, Dawoud RA, Hmed AA (2021) Characterization and full genome sequence of novel KPP-5 lytic phage against *Klebsiella pneumoniae* responsible for recalcitrant infection. Biomed 9:342. https://doi.org/10.3390/biomedicines9040342

Sonnhammer ELL, Eddy SR, Durbin R (1997) Pfam: a comprehensive database of protein domain families based on seed alignments. Proteins 28(3):405–420. https://doi.org/10.1002/(SICI)1097-0134(199707)28:3%3c405::AID-PROT10%3e3.0.CO;2-L

Stothard P (2000) The sequence manipulation suite: JavaScript programs for analyzing and formatting protein and DNA sequences. Biotech 28:1102–11024. https://doi.org/10.2144/00286ir01

Stummeyer K, Dickmanns A, Mühlenhoff M, Gerardy-Schahn R, Ficner R (2005) Crystal structure of the polysialic acid-degrading endosialidase of bacteriophage K1F. Nat Struct Mol Biol 12:90–96. https://doi.org/10.1038/nsmb874

Sullivan MJ, Petty NK, Beatson SA (2011) Easyfig: a genome comparison visualizer. Bioinforma 27:1009–1010. https://doi.org/10.1093/bioinformatics/btr039

Summer EJ, Berry J, Tran TAT, Niu L, Struck DK, Young R (2007) Rz/Rz1 lysis gene equivalents in phages of Gram-negative hosts. J Mol Biol 373:1098–1112. https://doi.org/10.1016/j.jmb.2007.08.045

Tan D, Gram L, Middelboe M (2014) Vibriophages and their interactions with the fish pathogen *Vibrio anguillarum*. Appl Environ Microbiol 80:3128–3140. https://doi.org/10.1128/AEM.03544-13

Taylor R, McDonald M, Russ G, Carson M, Lukaczynski E (1981) *Vibrio alginolyticus* peritonitis associated with ambulatory peritoneal dialysis. Bri Med J (Clin Res Ed) 283:275. https://doi.org/10.1136/bmj.283.6286.275

Tcherepanov V, Ehlers A, Upton C (2006) Genome annotation transfer utility (GATU): rapid annotation of viral genomes using a closely related reference genome. BMC Genomics 7:150. https://doi.org/10.1186/1471-2164-7-150

Thompson FL, Iida T, Swings J (2004) Biodiversity of *vibrios*. Microbiol Mol Biol Rev 68:403–431. https://doi.org/10.1128/MMBR.68.3.403-431.2004

Tridge (2020) 2020 Industry report: mackerel. Market Intelligence Team. https://cdn.tridge.com/market_report_report/b9/df/33/b9df33b49173bd0adce086ca6fa89c9e66cf2890/210122_Mackerel_Report.pdf. Accessed 20 June 2022

Trimble JJ, Murthy SC, Bakker A, Grassmann R, Desrosiers RC (1988) A gene for dihydrofolate reductase in a herpesvirus. Sci 239:1145–1147. https://doi.org/10.1126/SCIENCE.2830673

Walker PJ, Siddell SG, Lefkowitz EJ, Mushegian AR, Adriaenssens EM, Alfenas-Zerbini P, Davison AJ, Dempsey DM, Dutilh BE, García ML, Harrach B, Harrison RL, Hendrickson RC, Junglen S, Knowles NJ, Krupovic M, Kuhn JH, Lambert AJ, Łobocka M, Nibert ML, Oksanen HM, Orton RJ, Robertson DL, Rubino L, Sabanadzovic S, Simmonds P, Smith DB, Suzuki N, Van Dooerslaer K, Vandamme AM, Varsani A, Zerbini FM (2021) Changes to virus taxonomy and to the International Code of Virus Classification and Nomenclature ratified by the International Committee on Taxonomy of Viruses (2021). Arch Virol 166:2633–2648. https://doi.org/10.1007/s00705-021-05156-1

Wen C, Ai C, Lu S, Yang Q, Liao H, Zhou S (2022) Isolation and characterization of the lytic *Pseudoxanthomonas kaohsiungensi* phage PW916. Viruses 14:1709. https://doi.org/10.3390/v14081709

Willis SH, Kazmierczak KM, Carter RH, Rothman-Denes LB (2002) N4 RNA polymerase II, a heterodimeric RNA polymerase with homology to the single-subunit family of RNA polymerases. J Bacteriol 184:4952–4961. https://doi.org/10.1128/JB.184.18.4952-4961.2002

Wittmann J, Turner D, Millard AD, Mahadevan P, Kropinski AM, Adriaenssens EM (2020) From orphan phage to a proposed new family-the diversity of N4-Like viruses. Antibiot (Basel) 9:1–12. https://doi.org/10.3390/ANTIBIOTICS9100663

Wong CL, Sieo CC, Tan WS, Abdullah N, Hair-Bejo M, Abu J, Ho YW (2014) Evaluation of a lytic bacteriophage, Φ st1, for biocontrol of *Salmonella enterica* serovar Typhimurium in chickens. Int J Food Microbiol 172:92–101. https://doi.org/10.1016/j.ijfoodmicro.2013.11.034

Xie ZY, Hu CQ, Chen C, Zhang LP, Ren CH (2005) Investigation of seven *Vibrio* virulence genes among *Vibrio alginolyticus* and *Vibrio parahaemolyticus* strains from the coastal mariculture systems in Guangdong, China. Lett Applied Microbiol 41:202–207. https://doi.org/10.1111/j.1472-765X.2005.01688.x

Yang TC, Ortiz D, Yang Q, De Angelis RW, Sanyal SJ, Catalano CE (2017) Physical and functional characterization of a viral genome maturation complex. Biophy J 112:1551–1560. https://doi.org/10.1016/j.bpj.2017.02.041

Yazdi M, Bouzari M, Ghaemi EA (2018) Isolation and characterization of a lytic bacteriophage (vB_PmiS-TH) and its application in combination with ampicillin against planktonic and biofilm forms of *Proteus mirabilis* isolated from urinary tract infection. J Mol Microbiol Biotechnol 28:37–46. https://doi.org/10.1159/000487137

Zadik PM, Chapman PA, Siddons CA (1993) Use of tellurite for the selection of verocytotoxigenic *Escherichia coli* O157. J Med Microbiol 39:155–158. https://doi.org/10.1099/00222615-39-2-155

Zhang KY, Gao YZ, Du MZ, Liu S, Dong C, Guo FB (2019) Vgas: a viral genome annotation system. Front Microbiol 10:184. https://doi.org/10.3389/fmicb.2019.00184

Zhang Y, Ding Y, Li W, Zhu W, Wang J, Wang X (2021) Application of a novel lytic *Podoviridae* phage Pu20 for biological control of drug-resistant *Salmonella* in liquid eggs. Pathog 10:34. https://doi.org/10.3390/pathogens10010034

Zivanovic Y, Confalonieri F, Ponchon L, Lurz R, Chami M, Flayhan A, Renouard M, Huet A, Decottignies P, Davidson AR, Breyton C, Boulanger P (2014) Insights into bacteriophage T5 structure from analysis of its morphogenesis genes and protein components. J Virol 88:1162–1174. https://doi.org/10.1128/JVI.02262-13

Authors and Affiliations

Sofiah Tajuddin[1] · Asif M. Khan[2,3] · Li Chuin Chong[2] · Chuan Loo Wong[1] · Jia Sen Tan[1] · Md Yasin Ina-Salwany[4,5] · Han Yih Lau[6] · Kok Lian Ho[7] · Abdul Razak Mariatulqabtiah[8,9] · Wen Siang Tan[1,9]

Sofiah Tajuddin
sofiahtajuddin95@gmail.com

[1] Department of Microbiology, Faculty of Biotechnology and Biomolecular Sciences, Universiti Putra Malaysia, Selangor 43400 UPM Serdang, Malaysia

[2] Centre for Bioinformatics, School of Data Sciences, Perdana University, 50490 Kuala Lumpur, Malaysia

[3] Beykoz Institute of Life Sciences and Biotechnology, Bezmialem Vakif University, Beykoz, 34820 Istanbul, Turkey

[4] Department of Aquaculture, Faculty of Agriculture, Universiti Putra Malaysia, Selangor 43400 UPM Serdang, Malaysia

[5] Aquatic Animal Health and Therapeutics Laboratory, Institute of Bioscience, Universiti Putra Malaysia, Selangor 43400 UPM Serdang, Malaysia

[6] Biotechnology and Nanotechnology Research Centre, Malaysian Agricultural Research and Development Institute (MARDI), 43400 Serdang, Malaysia

[7] Department of Pathology, Faculty of Medicine and Health Sciences, Universiti Putra Malaysia, Selangor 43400 UPM Serdang, Malaysia

[8] Department of Cell and Molecular Biology, Faculty of Biotechnology and Biomolecular Sciences, Universiti Putra Malaysia, Selangor 43400 UPM Serdang, Malaysia

[9] Laboratory of Vaccine and Biomolecules, Institute of Bioscience, Universiti Putra Malaysia, Selangor 43400 UPM Serdang, Malaysia